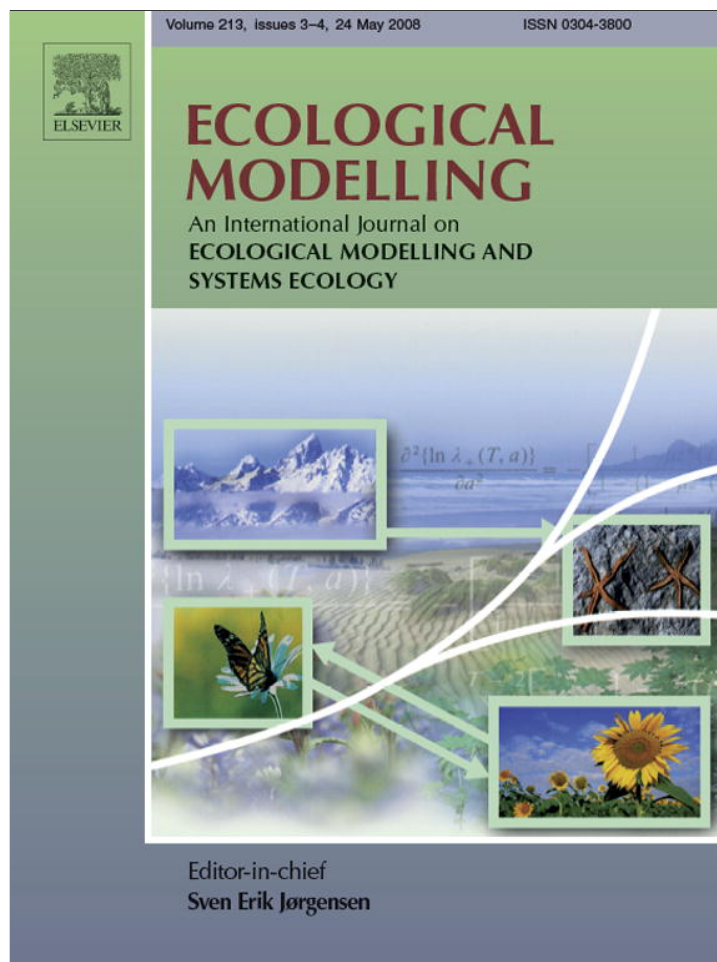


Provided for non-commercial research and education use.
Not for reproduction, distribution or commercial use.



This article appeared in a journal published by Elsevier. The attached copy is furnished to the author for internal non-commercial research and education use, including for instruction at the authors institution and sharing with colleagues.

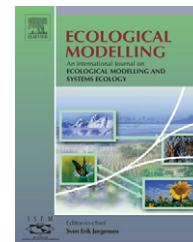
Other uses, including reproduction and distribution, or selling or licensing copies, or posting to personal, institutional or third party websites are prohibited.

In most cases authors are permitted to post their version of the article (e.g. in Word or Tex form) to their personal website or institutional repository. Authors requiring further information regarding Elsevier's archiving and manuscript policies are encouraged to visit:

<http://www.elsevier.com/copyright>



ELSEVIER

available at www.sciencedirect.comjournal homepage: www.elsevier.com/locate/ecolmodel

Plankton community patterns across a trophic gradient: The role of zooplankton functional groups

Jingyang Zhao, Maryam Ramin, Vincent Cheng, George B. Arhonditsis*

Department of Physical & Environmental Sciences, University of Toronto, Toronto, Ontario, Canada M1C 1A4

ARTICLE INFO

Article history:

Received 27 August 2007

Received in revised form

6 January 2008

Accepted 15 January 2008

Published on line 5 March 2008

Keywords:

Zooplankton community

Complex mathematical models

Stoichiometric theory

Resource competition

Algal food quality

Nutrient recycling

ABSTRACT

We use a complex aquatic biogeochemical model to examine competition patterns and structural shifts in plankton communities under nutrient enrichment conditions. Our model simulates multiple elemental cycles (organic C, N, P, Si, O), multiple functional phytoplankton (diatoms, green algae and cyanobacteria) and zooplankton (copepods and cladocerans) groups. The model provided a realistic platform to examine the functional properties (e.g., grazing strategies, food quality, predation rates, stoichiometry, basal metabolism, and temperature requirements) and the abiotic conditions (temperature, nutrient loading) under which the different plankton groups can dominate or can be competitively excluded in oligo-, meso- and eutrophic environments. Our analysis shows that the group-specific maximum grazing rates, the predation rates from planktivorous fish, along with the temperature requirements to attain optimal growth can be particularly influential on the structure of plankton communities. The model also takes into account recent advances in stoichiometric nutrient recycling theory, which allowed examining the effects of the cyanobacteria food quality, the critical threshold for mineral P limitation, and the half saturation constant for assimilation efficiency on the zooplankton functional group biomass across a range of nutrient loading conditions. Our study highlights the adverse effects that the cyanobacteria food quality can have on the two functional zooplankton groups in productive systems, despite the differences in their feeding selectivity strategies, i.e., cladocerans are filter-feeders with equal preference among the different types of food, whereas copepods are assumed to be capable of selecting on the basis of food quality. Finally, we conclude that the articulate representation of the producer–grazer interactions using stoichiometrically/biochemically realistic terms will offer insights into the patterns of nutrient and energy flow transferred to the higher trophic levels.

© 2008 Elsevier B.V. All rights reserved.

1. Introduction

The central role of herbivory in shaping the structure of plankton communities (i.e., competitive exclusion or species coexistence mediated by herbivores, evolution of the phytoplankton growth strategies induced by grazing selectivity) and in linking the standing biomass of algae with fish

populations has been extensively highlighted in aquatic ecology (Lampert and Sommer, 1997; Grover, 1997). Despite the tremendous effort and a wide variety of approaches devoted to studying this topic, the drivers of the variability at the phytoplankton–zooplankton interface remain controversial and arguably only partially understood (Lehman, 1988; Brett and Goldman, 1997; Polis et al., 2000). A recent meta-analysis

* Corresponding author. Tel.: +1 416 208 4858; fax: +1 416 287 7279.

E-mail address: georgea@utsc.utoronto.ca (G.B. Arhonditsis).

0304-3800/\$ – see front matter © 2008 Elsevier B.V. All rights reserved.

doi:10.1016/j.ecolmodel.2008.01.016

of 153 aquatic biogeochemical modelling studies provided evidence that zooplankton dynamics is the most poorly predicted component of planktonic systems (Arhonditsis and Brett, 2004). Specifically, the median relative error from approximately thirty zooplankton simulations was 70%, and more than a quarter of the studies reported error higher than 100% (see Fig. 3 and Table 1 in Arhonditsis and Brett, 2004). Although these results can partly be explained by the paucity of zooplankton data and the error associated with converting the collected information (in units of individuals per volume) to the modelled units (usually carbon or nitrogen mass per volume), the considerable model misfit mainly stems from our inability to mathematically depict the behavioural complexities, the idiosyncrasies of metabolic regulation, and the diverse patterns of somatic growth and reproduction of zooplankton communities (Fennel and Neumann, 2001; Franks, 2002).

A typical thorny issue in food web modelling is the optimal aggregation level of the zooplankton community, where the existing strategies span a very wide range of complexity. Early aquatic biogeochemical models typically regarded zooplankton as an aggregated biotic entity and parameterized bulk properties such as grazing rates, assimilation efficiency, metabolic strategies, and consumer-driven nutrient recycling (McGillicuddy et al., 1995; Doney et al., 1996; Arhonditsis et al., 2000; Franks and Chen, 2001). These studies mainly aimed to quantify the transfer of mass and energy among trophic levels, to address local management issues (e.g., eutrophication control), and to understand the interplay between hydrodynamic patterns and mesoscale nutrient and plankton distributions in oceanic systems. On the other hand, there are ecological questions that require more sophisticated formulations and higher resolution of the zooplankton compartment (Broekhuizen et al., 1995; Fennel and Neumann, 2001; Arhonditsis and Brett, 2005a). For example, the explicit consideration of smaller and larger size zooplankton classes allows to more realistically assess the connections between the ocean's carbon cycle and global climatic variability (i.e., the "biological pump"), and insights into the plankton succession patterns in epilimnetic environments can only be gained by distinguishing among different functional groups (e.g., copepods, cladocerans). Other authors have also pointed out that the only effective way to predict zooplankton dynamics is to fully simulate zooplankton life histories, e.g., the copepod-submodel suggested by Fennel (2001) that included eggs, nauplii, copepodites and adults as state variables.

Another topic that has received considerable attention is the mathematical representation of the biochemical heterogeneity at the primary producer–grazer interface to illuminate the patterns of nutrient and energy flow transferred through the food web (Andersen, 1997; Loladze et al., 2000; Arhonditsis and Brett, 2005a; Mulder and Bowden, 2007). The aquatic ecology literature suggests that the algal taxonomic differences in food quality due to differences in their highly unsaturated fatty acid (HUFA), protein, amino acid content, and/or digestibility determine the strength of the trophic coupling in aquatic pelagic food webs, e.g., HUFA bottom-up hypothesis (Brett and Muller-Navarra, 1997; Muller-Navarra et al., 2004). Other studies underscore the importance of the constraints imposed from the mass balance of multiple chemical

elements (C, N, P) on ecological interactions pinpointing the critical role of the discrepancy between the prey and predator elemental somatic ratios on food web structure and pelagic ecosystem functioning (Elser and Urabe, 1999). In this regard, our theoretical understanding has advanced from a series of stoichiometric models that account for the effects of P-deficient food on the rate of P zooplankton recycling by explicitly considering animal demands (e.g., respiration, biomass production) for both C and P (e.g., Hessen and Andersen, 1992; Andersen, 1997). The Loladze et al. (2000) and Mulder and Bowden (2007) modelling studies are two characteristic examples with particularly intriguing findings that need to be tested in real world conditions. Loladze et al. (2000) modified the Rosenzweig-MacArthur variation of the Lotka-Volterra equations and demonstrated that the chemical heterogeneity in the first two trophic levels can result in interesting dynamic behaviour under nutrient limiting conditions; in particular, the two biotic compartments (prey and predator) can be transformed into competitors for phosphorus and their interactions shift from the typical (+, –) class to the paradoxical (–, –) type. Mulder and Bowden (2007) relaxed the assumption of strict homeostasis of the grazer and showed that variable zooplankton stoichiometry allows overcoming poor food quality limitations in high-energy, low-nutrient environments.

In this study, we use a complex aquatic biogeochemical model to examine competition patterns and structural shifts in the plankton community across a trophic gradient. Our model simulates multiple elemental cycles (organic C, N, P, Si, O), multiple functional phytoplankton (diatoms, green algae and cyanobacteria) and zooplankton (copepods and cladocerans) groups. The model provides a realistic platform to examine the functional properties (e.g., grazing strategies, food quality, predation rates, stoichiometry, basal metabolism, and temperature requirements) and the abiotic conditions (temperature, nutrient loading) under which the different plankton groups can dominate or can be competitively excluded in oligo-, meso- and eutrophic environments. Finally, our study attempts to elucidate aspects of the zooplankton feeding and growth efficiency modelling strategies by assessing the effects of the cyanobacteria food quality, the critical threshold for mineral P limitation, and the half saturation constant for growth efficiency on the zooplankton functional group biomass across a wide range of nutrient loading conditions.

2. Methods

2.1. Aquatic biogeochemical model

2.1.1. Model description

The spatial structure of the model is composed of two compartments representing the epilimnion (upper layer) and hypolimnion (lower layer) of a lake. The model simulates five biogeochemical cycles, i.e., organic carbon, nitrogen, phosphorus, silica and dissolved oxygen. The particulate phase of the elements is represented from the state variables particulate organic carbon, particulate organic nitrogen, particulate organic phosphorus, and particulate silica. The dissolved

phase fractions comprise the dissolved organic (carbon, nitrogen, and phosphorus) and inorganic (nitrate, ammonium, phosphate, silica, and oxygen) forms involved in the five elemental cycles. The major sources and sinks of the particulate forms include plankton basal metabolism, egestion of excess particulate matter during zooplankton feeding, settling to the hypolimnion or sediment, bacterial-mediated dissolution, external loading, and loss with outflow. Similar processes govern the levels of the dissolved organic and inorganic forms as well as the bacterial mineralization and the vertical diffusive transport. The model also explicitly simulates denitrification, nitrification, heterotrophic respiration, and the water column-sediment exchanges. The external forcing encompasses river inflows, precipitation, evaporation, solar radiation, water temperature, and nutrient loading. The reference conditions for our Monte Carlo analysis correspond to the average epilimnetic/hypolimnetic temperature, solar radiation, and vertical diffusive mixing in Lake Washington (Arhonditsis and Brett, 2005b; Brett et al., 2005). Similar strategy was also followed with regards to the reference conditions for the hydraulic and nutrient loading. Specifically, the hydraulic renewal rate in our hypothetical system is 0.384 year^{-1} . The fluvial and aerial total nitrogen inputs are $1114 \times 10^3 \text{ kg year}^{-1}$, and the exogenous total phosphorus loading contributes approximately $74.9 \times 10^3 \text{ kg year}^{-1}$. The exogenous total organic carbon supplies to the system are $6685 \times 10^3 \text{ kg year}^{-1}$. In our analysis, the average input nutrient concentrations for the oligo-, meso-, and eutrophic environments correspond to 50% (2.9 mg TOC/L, 484 $\mu\text{g TN/L}$ and 32.5 $\mu\text{g TP/L}$), 100% (5.8 mg TOC/L, 967 $\mu\text{g TN/L}$ and 65 $\mu\text{g TP/L}$), and 200% (11.6 mg TOC/L, 1934 $\mu\text{g TN/L}$ and 130 $\mu\text{g TP/L}$) of the reference conditions, respectively.

Detailed model description has been provided in Arhonditsis and Brett (2005a); therefore, our focus herein is on the model equations related to zooplankton dynamics (Table 1).

The herbivorous zooplankton biomass in this study is controlled by growth, basal metabolism, higher predation, and outflow losses. The zooplankton grazing term explicitly considers algal food quality effects on zooplankton assimilation efficiency, and also takes into account recent advances in stoichiometric nutrient recycling theory (Arhonditsis and Brett, 2005a). We used a dynamic approach to model the effects of both ingested food quality and quantity on zooplankton phosphorus production efficiency (Arhonditsis and Brett, 2005a; Mulder and Bowden, 2007). First, we introduced a variable that is referred to as “food quality concentration” (FQ) and is the product of two terms: (a) the first term is the sum of the four food-type (diatoms, green algae, cyanobacteria and detritus) concentrations (square roots) weighted by the respective qualities, expressed by a food quality index that varies from 0 to 1, and (b) the second term reflects the assumption that the total food quality decreases by a factor directly proportional to the imbalance between the C:P ratio of the grazed seston ($\text{Graz}_{C/P}$) and a critical C:P₀ ratio above which zooplankton growth will be limited by P availability.

$$FQ_{(j)} = \left(\sum_{i=\text{diat. green. cyano}} FQ_{(i,j)} \sqrt{\text{PHYT}_{(i)}} + FQ_{\text{det}(j)} \sqrt{\text{POC}} \right) \times \text{ZOOP}_{C/PLIM(j)} \quad (1)$$

Table 1 – Definitions and statistical distributions of 17 model parameters pertaining to zooplankton dynamics

Model parameter	Symbol	Unit measurement	Cladocerans	Copepods	Sources
Maximum grazing rate	grazing _{max}	day ⁻¹	N(0.8, 0.086 ²)	N(0.45, 0.043 ²)	1–5
Half saturation constant for grazing	KZ	mg C m ⁻³	N(110, 12.9 ²)	N(95, 10.7 ²)	1, 2
Quality as a food of diatoms	FQ _{diat}	–	N(0.85, 0.064 ²)	N(0.85, 0.064 ²)	6, 7
Quality as a food of green algae	FQ _{greens}	–	N(0.7, 0.043 ²)	N(0.7, 0.043 ²)	6, 7
Quality as a food of cyanobacteria	FQ _{cyano}	–	N(0.0, 0.215 ²)	N(0.0, 0.215 ²)	6, 7
Quality as a food of detritus	FQ _{det}	–	N(0.5, 0.064 ²)	N(0.5, 0.064 ²)	6–8
Critical threshold for mineral P limitation	C:P ₀	mg C mg P ⁻¹	N(116, 12.5 ²)	N(116, 12.5 ²)	6
Half saturation constant for zooplankton growth efficiency	ef ₂	(mg C m ⁻³) ^{1/2}	N(17.5, 1.08 ²)	N(19.5, 1.08 ²)	9
Specific zooplankton predation rate	pred ₁	day ⁻¹	N(0.15, 0.021 ²)	N(0.15, 0.021 ²)	10–12
Half saturation constant for predation	pred ₂	mg C m ⁻³	N(40, 8.6 ²)	N(40, 8.6 ²)	10–12
Basal metabolism rate	bm _{ref}	day ⁻¹	N(0.06, 0.009 ²)	N(0.05, 0.009 ²)	1–5, 13
Effects of temperature on zooplankton metabolism	ktbm	°C ⁻¹	N(0.10, 0.009 ²)	N(0.05, 0.009 ²)	4, 13
Carbon to nitrogen somatic ratio	C/N	mg C mg N ⁻¹	N(7, 0.4 ²)	N(5, 0.4 ²)	14, 15
Carbon to phosphorus somatic ratio	C/P	mg C mg P ⁻¹	N(35, 2.1 ²)	N(50, 2.1 ²)	14, 15
Optimal temperature for zooplankton grazing	T _{opt}	°C	U(19, 21)	U(17, 18.5)	3, 4, 13, 16, 17
Effects of temperature below T _{opt}	KTgr1	°C ⁻²	U(0.01, 0.02)	U(0.001, 0.005)	3, 4, 13, 16, 17
Effects of temperature above T _{opt}	KTgr2	°C ⁻²	U(0.01, 0.02)	U(0.001, 0.005)	3, 4, 13, 16, 17

(1) Sommer (1989); (2) Jorgensen et al. (1991); (3) Lampert and Sommer (1997); (4) Wetzel (2001); (5) Chen et al. (2002) (and references therein); (6) Brett et al. (2000) (and references therein); (7) Park et al. (2002); (8) Ederington et al. (1995); (9) Arhonditsis and Brett (2005a); (10) Fasham (1993); (11) Malchow (1994); (12) Ross et al. (1994); (13) Omlin et al. (2001); (14) Hessen and Lyche (1991); (15) Sterner et al. (1992); (16) Orcutt and Porter (1983); (17) Downing and Rigler (1984).

$$ZOO_{C/PLIM(j)} = \begin{cases} \text{Graz}_{C/P(j)} \leq C : P_0 & 1 \\ \text{Graz}_{C/P(j)} > C : P_0 & \frac{C : P_0}{\text{Graz}_{C/P(j)}} \end{cases} \quad (2)$$

$$\text{Graz}_{C/P(j)} = \frac{\sum_{i=\text{diat, green, cyan}} \text{grazing}_{\text{max}(j)} \text{pref}_{(i,j)} \text{PHYT}_{(i)} + \text{grazing}_{\text{max}(j)} \text{pref}_{\text{det}(j)} \text{POC}}{\sum_{i=\text{diat, green, cyan}} \text{grazing}_{\text{max}(j)} \text{pref}_{(i,j)} \text{PHYT}_{(i)} P_{(i)} + \text{grazing}_{\text{max}(j)} \text{pref}_{\text{det}(j)} \text{POP}} \quad j = \text{clad, cop} \quad (3)$$

$$\text{pref}_{(i,j)} = \frac{\text{pref}_{0(i,j)} \text{FOOD}_i}{\sum_{i=\text{diat, green, cyan, det}} \text{pref}_{0(i,j)} \text{FOOD}_i} \quad (4)$$

where $\text{pref}_{0(i,j)}$ represents the nominal preference of the zooplankton group j for the food-type i ; and FOOD_i is the concentration of the four food-types, i.e., diatoms, green algae, cyanobacteria, and detritus. The weighting scheme of the first term considers differences in food quality other than the P content, and accounts for biochemical/morphological characteristics of the four food-types. For example, it can characterize algal taxonomic differences in food quality due to differences in their highly unsaturated fatty acid (HUFA), amino acid, protein content and/or digestibility (Sterner and Hessen, 1994; Kilham et al., 1997; Kleppel et al., 1998; Brett and Muller-Navarra, 1997; Muller-Navarra et al., 2000). This expression assumes that below the critical seston C:P threshold, the food concentration and biochemical composition solely determines zooplankton growth efficiency. Above the critical C:P threshold mineral P limitation is an additional factor that can influence food quality.

We used a hyperbolic formula (for example, see the conceptual diagram in Figure 4.28 of Lampert and Sommer, 1997) to relate the phosphorus production efficiency with the variable food quality concentration:

$$\text{gref}_{P(j)} = \frac{ef_{1(j)} \text{FQ}_{(j)}}{ef_{2(j)} + \text{FQ}_{(j)}} \quad (5)$$

Under the assumption of strict homeostasis, the carbon and nitrogen use efficiencies are given by:

$$\text{gref}_{C(j)} = \frac{C/P_{ZOO} \text{gref}_{P(j)} \left(\sum_{i=\text{diat, green, cyan}} \text{grazing}_{\text{max}(j)} \text{pref}_{(i,j)} \text{PHYT}_{(i)} P_{(i)} + \text{grazing}_{\text{max}(j)} \text{pref}_{\text{det}(j)} \text{POP} \right)}{\sum_{i=\text{diat, green, cyan}} \text{grazing}_{\text{max}(j)} \text{pref}_{(i,j)} \text{PHYT}_{(i)} + \text{grazing}_{\text{max}(j)} \text{pref}_{\text{det}(j)} \text{POC}} \quad (6)$$

$$\text{gref}_{N(j)} = \frac{N/P_{ZOO} \text{gref}_{P(j)} \left(\sum_{i=\text{diat, green, cyan}} \text{grazing}_{\text{max}(j)} \text{pref}_{(i,j)} \text{PHYT}_{(i)} P_{(i)} + \text{grazing}_{\text{max}(j)} \text{pref}_{\text{det}(j)} \text{POP} \right)}{\sum_{i=\text{diat, green, cyan}} \text{grazing}_{\text{max}(j)} \text{pref}_{(i,j)} \text{PHYT}_{(i)} N_{(i)} + \text{grazing}_{\text{max}(j)} \text{pref}_{\text{det}(j)} \text{PON}} \quad (7)$$

The two zooplankton functional groups (cladocerans and copepods) differ with regards to their grazing rates, food preferences, selectivity strategies, elemental somatic ratios, vulnerability to predators, and temperature requirements (Arhonditsis and Brett, 2005a,b). Cladocerans are modelled as filter-feeders with an equal preference among the four food-types (diatoms, green algae, cyanobacteria, detritus), high maximum grazing rates and metabolic losses, lower half saturation for growth efficiency, high temperature optima and high sensitivity on low temperatures, low nitrogen and high phosphorus content. In contrast, copepods are characterized by lower maximum grazing and metabolic rates, capability of selecting on the basis of food qual-

ity, higher feeding rates at low food abundance, slightly higher nitrogen and much lower phosphorus content, lower temperature optima with a wider temperature tolerance. Fish predation on cladocerans is modelled by a sigmoidal function, while a hyperbolic form is adopted for copepods

(Edwards and Yool, 2000). Both forms exhibit a plateau at high zooplankton concentrations representing satiation of the fish predation, e.g., the fish can only process a certain number of food items per unit time or there is a maximum limit on predator density caused by direct interference among the predators themselves. The S-shaped curve, however, is more appropriate for reproducing the tight connection between planktivorous fish and large *Daphnia* adults at higher zooplankton densities, due to fish specialisation (learning ability of fish to capture large animals) or lack of escape behaviour of the prey (Lampert and Sommer, 1997).

The phytoplankton community consists of three functional groups, i.e., diatoms, green algae, and cyanobacteria, and their production and losses are governed by growth, basal metabolism, herbivorous zooplankton grazing, settling to sediment or hypolimnion, epilimnion/hypolimnion diffusion exchanges, and outflow losses. Nutrient, light, and temperature effects on phytoplankton growth are considered using a multiplicative model (Jorgensen and Bendricchio, 2001). The three phytoplankton groups modelled differ with regards to their strategies for resource competition (nitrogen, phosphorus, light, temperature) and metabolic rates as well as their morphological features (settling velocity, shading effects); in addition, they differ on the feeding preference and food quality for herbivorous zooplankton (Arhonditsis and Brett, 2005a,b). These differences drive their competition patterns along with their interplay with the zooplankton community.

2.1.2. Model application

Our Monte Carlo analysis examines the functional properties (e.g., grazing strategies, stoichiometry and food selectivity)

and the abiotic conditions (temperature, nutrient loading) under which the zooplankton succession patterns will be manifested in oligo-, meso- and eutrophic environments (Fig. 1). Based on the previous characterization of the two functional groups, we assigned probability distributions that reflect our knowledge (field observations, laboratory studies, literature information and expert judgment) on the relative plausibility of their grazing strategies, basal metabolism, food quality, stoichiometry (C, N, P), predation rates, and temperature requirements (Table 1). In this study, we used the following protocol to formulate the parameter distributions: (i) we identified the global (not the group-specific) minimum and maximum values for each parameter from the pertinent

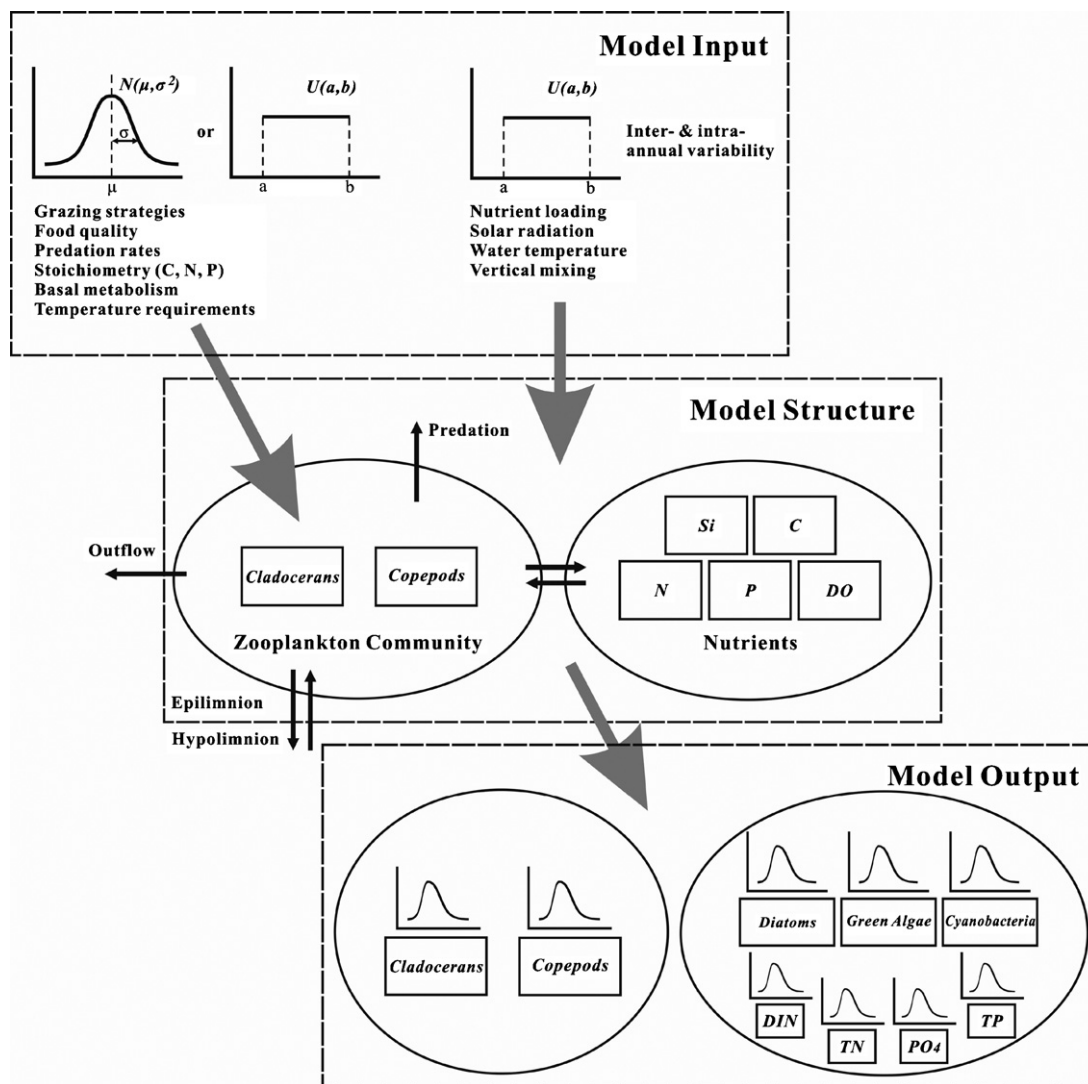


Fig. 1 – Monte Carlo analysis of the aquatic biogeochemical model. The input vector consists of forcing functions (i.e., nutrient loading, solar radiation, epilimnion temperature, hypolimnion temperature, and epilimnion/hypolimnion vertical mixing) and functional properties (i.e., grazing strategies, food quality, predation rates, stoichiometry, basal metabolism, and temperature requirements) of the two zooplankton groups.

literature; (ii) we subdivided the original parameter space into two subregions reflecting the functional properties of the zooplankton groups; and then (iii) we assigned normal or uniform distributions parameterized such that 98% of their values were lying within the identified ranges. The group-specific parameter spaces were also based on the calibration vector presented during the model application in Lake Washington (see Appendix B in Arhonditsis and Brett, 2005a). For example, the identified range for the maximum zooplankton grazing rate was $0.35\text{--}1.00\text{ day}^{-1}$, while the two subspaces were $0.45 \pm 0.10\text{ day}^{-1}$ for copepods (calibration value \pm literature range) and $0.80 \pm 0.20\text{ day}^{-1}$ for cladocerans. We then assigned normal distributions formulated such that 98% of their values were lying within the specified ranges. We also introduced perturbations of the reference abiotic conditions, uniformly sampled from the range $\pm 20\%$, to accommodate the inter-annual variability associated with nutrient loading, solar radiation, epilimnetic/hypolimnetic temperature, and vertical

diffusion. In a similar manner, we incorporated daily noise representing the intra-annual abiotic variability (Arhonditsis and Brett, 2005b). For each trophic state, we generated 7000 input vectors independently sampled from 32 (27 model parameters and 5 forcing functions) probability distributions, which were used to run the model for 10 years. Finally, we produced three ($7000 \times 12 \times 9$) output matrices that comprised the average monthly epilimnetic values for the five plankton functional group biomass, dissolved inorganic nitrogen (DIN), total nitrogen (TN), phosphate (PO_4), and total phosphorus (TP) concentrations in the oligo-, meso-, and eutrophic environments.

2.2. Statistical analysis

2.2.1. Principal component analysis and multiple linear regression models

Principal component analysis (PCA), a data reduction and structure detection technique (Legendre and Legendre, 1998),

was applied for identifying different modes of intra-annual variability (Jassby, 1999; Arhonditsis et al., 2004). The basic rationale behind this application of PCA is that different phases of the intra-annual cycle may be regulated by distinct mechanisms and may therefore behave independently of each other, thereby hampering the identification of clear cause–effect relationships (Jassby, 1999). For each zooplankton functional group, the monthly biomass matrix of 12 columns (months of the year) and 7000 rows (output data sets) was formed for each trophic state. PCA was used to unravel the number of independent modes of biomass variability, and the months of year in which they were most important (component coefficients). Principle components (PCs) were estimated by singular value decomposition of the covariance matrix. The selection of significant PCs was based on the Kaiser criterion which means that we retained only PCs with eigenvalues greater than 1, i.e., a factor is considered only if the variability explained is greater than the equivalent of one original variable. The significant modes were rotated using the normalized varimax strategy to calculate the new component coefficients (Richman, 1986). We then developed multiple linear regression models within the resultant seasonal modes of variability, whereas when a pair functional group-trophic state did not result in the extraction of significant PCs the multiple regression analysis was implemented for each month. We employed a forward-stepwise parameter selection scheme using as predictors the functional properties and abiotic conditions considered in our Monte Carlo analysis.

2.2.2. Classification trees

Classification trees were used to predict responses of a categorical dependent variable (i.e., zooplankton functional groups) based on one or more independent predictor variables (i.e., model parameters and forcing functions), without specifying *a priori* the form of their interactions (Breiman et al., 1984; De'ath and Fabricius, 2000). For each functional group, we considered the July average biomass classified by lumping every $35 \mu\text{g C L}^{-1}$ as one class (e.g., 0–35, 35–70, and so on) to convert continuous biomass data into categorical data. The predictor variables consist of the group-specific model parameters, the abiotic conditions, and the levels of the rest state variables in July. The outputs from the three trophic states were combined to obtain a matrix of 21,000 rows for the classification tree analysis. During the analysis, the algorithm began with the root (or parent) node, which corresponded to the original categorical data for each zooplankton functional group. The data were split into increasingly homogeneous subsets with binary recursive partitioning and examination of all possible splits for each predictor variable at each node, until the Gini measure of node impurity was below a pre-specified baseline (Breiman et al., 1984). The stopping rule for the analysis was that the terminal nodes (also known as leaves in the tree analogy) should not contain more cases than 5% of the size of each class. The final classification trees represented a hierarchical structure (shown as dendrograms) illustrating the interplay among physical, chemical and biological factors that drives structural shifts in zooplankton communities, i.e., different levels of each zooplankton functional group (nodes) were associated with threshold values of its functional properties (e.g., grazing strategies, metabolic rates, stoichiometry) along with

critical levels of the abiotic conditions, the three residents of the phytoplankton community or the other zooplankton competitor (splitting conditions).

3. Results

3.1. Statistical results of the Monte Carlo analysis

The summary statistics of the major limnological variables in the three trophic states, as derived from averaging the model endpoints over the 10-year simulation period, are given in Table 2. The average annual phosphate (PO_4) and total phosphorus (TP) concentrations increase by nearly 180% from the oligotrophic to the eutrophic environment, whereas the corresponding dissolved inorganic nitrogen (DIN) and total nitrogen (TN) increase was relatively lower ($\leq 95\%$). The total nitrogen to total phosphorus ratio (TN/TP) supports stoichiometric predictions of phosphorus limitations in the three environments. However, the transition from the oligotrophic to the eutrophic state is associated with a relaxation of the phosphorus limitation as the TN/TP declines from 21.3 to 15.2; in fact, the latter environment lies at the dichotomy boundary (Redfield ratio 16:1) between phosphorus and nitrogen limitation, while several Monte Carlo simulations represented nitrogen limiting conditions (see reported ranges in Table 2). In general, the phytoplankton biomass shows an increasing trend in response to the nutrient enrichment and the chlorophyll *a* concentrations increase from 3.1 to $5.0 \mu\text{g chl a L}^{-1}$. Diatoms possess superior phosphorus kinetics and therefore consistently dominate the phytoplankton community, accounting for 55, 45, and 40% of the total phytoplankton biomass at the three trophic states, respectively. Being the intermediate competitors, green algae contribute approximately 30% to the composition of phytoplankton, whereas the cyanobacteria proportion was relatively low ($\leq 30\%$) due to their phosphorus competitive handicap. In response to the phytoplankton biomass increase, the biomass of the two zooplankton groups progressively rises across the three trophic states and the two groups demonstrate an approximately 2.5-fold increase. Both cladocerans and copepods respond to the spring phytoplankton bloom and reach their annual maxima in May, whereas another secondary cladoceran peak is observed in July in the eutrophic environment (Fig. 2). As nutrient loading increases, the median spring values of the cladoceran and copepod biomass increase from 93.9 and 65.3 to 209.8 and $153.7 \mu\text{g C L}^{-1}$, respectively. Cladocerans are the dominant zooplankton group during the summer-stratified period, while copepods due to their tolerance to low temperatures have competitive advantage throughout the winter–early spring period and also have the ability to promptly respond to the initiation of the spring phytoplankton bloom.

3.2. Principle component analysis and multiple linear regression models

The PCA analysis revealed the existence of two or three distinct modes of variability characterizing the temporal patterns of cladocerans at the three trophic states (Fig. 3). On the other hand, two significant PCs pertaining to copepod intra-

Table 2 – Monte Carlo analysis of the model in three trophic states

	PO ₄ (µg L ⁻¹)	TP (µg L ⁻¹)	DIN (µg L ⁻¹)	TN (µg L ⁻¹)	TN/TP	Chla (µg L ⁻¹)	DB (µg Chla L ⁻¹)	GB (µg Chla L ⁻¹)	CYB (µg Chla L ⁻¹)	CLB (µg CL ⁻¹)	COB (µg CL ⁻¹)
Oligotrophic											
Mean	6.5	13.7	165	291	21.3	3.1	1.7	0.9	0.5	29.0	17.9
Median	6.4	13.6	164	290	21.3	3.1	1.6	0.9	0.5	28.8	17.2
Int. range	1.3	1.8	19	20	1.9	0.5	0.4	0.1	0.1	10.4	9.8
Min	4.4	10.4	111	245	16.4	1.9	0.8	0.6	0.2	1.6	0.7
Max	12.9	21.2	223	347	27.3	4.8	3.2	1.3	0.8	60.0	49.9
Mesotrophic											
Mean	9.8	21.0	188	376	18.0	4.0	1.9	1.2	0.9	43.6	30.3
Median	9.6	20.7	187	375	18.1	4.0	1.8	1.2	0.9	43.7	28.7
Int. range	2.2	2.6	29	26	1.5	0.7	0.5	0.2	0.2	14.4	15.6
Min	6.0	16.1	119	322	13.2	2.4	1.0	0.7	0.6	7.4	3.4
Max	20.4	33.0	272	446	22.2	6.1	3.6	1.8	1.5	81.5	89.4
Eutrophic											
Mean	18.1	37.3	268	560	15.2	5.0	2.0	1.5	1.5	68.6	50.1
Median	17.3	36.5	266	559	15.3	5.0	2.0	1.5	1.5	69.5	47.7
Int. range	5.1	6.3	49	41	1.8	1.1	0.6	0.3	0.3	21.3	26.4
Min	10.2	26.8	169	483	10.4	2.2	0.8	0.7	0.7	17.0	9.4
Max	41.9	63.6	445	678	19.7	7.9	3.9	2.3	2.2	112.6	129.6

Summary statistics of the average annual values of the phosphate (PO₄), total phosphorus (TP), dissolved inorganic nitrogen (DIN), total nitrogen (TN), ratio of total nitrogen to total phosphorus (TN/TP), chlorophyll *a* (Chla), diatom biomass (DB), green algae biomass (GB), cyanobacteria biomass (CYB), cladoceran biomass (CLB), and copepod biomass (COB). Mean: average value; Int. range: interquartile range (difference between the 75th and 25th percentiles); Median: median value; Max: maximum value; Min: minimum value.

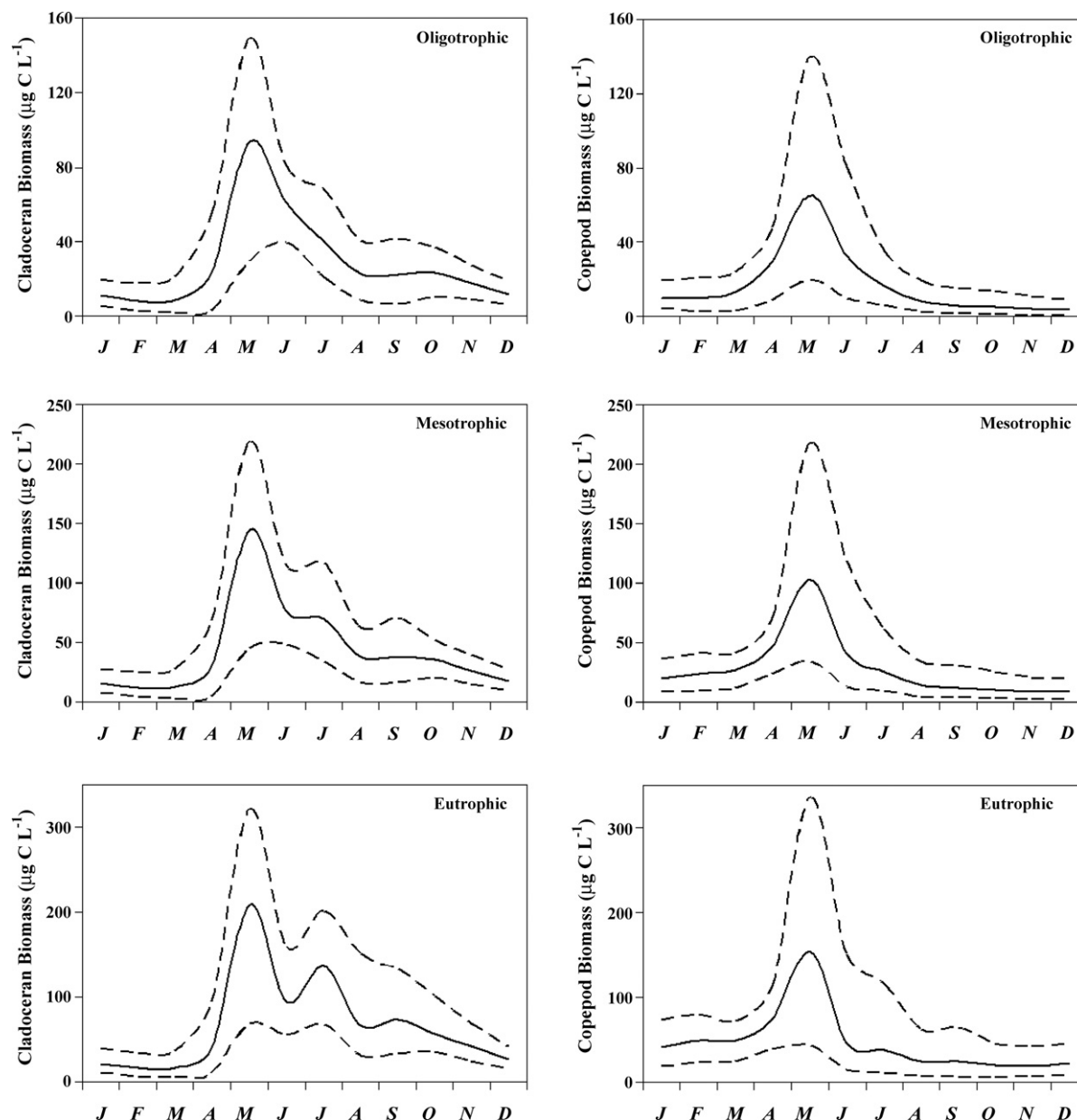


Fig. 2 – Seasonal variability of two zooplankton functional groups (i.e., cladocerans and copepods) across a trophic gradient ((a) oligotrophic; (b) mesotrophic; (c) eutrophic). Solid lines correspond to monthly median biomass values; dashed lines correspond to the 2.5 and 97.5th percentile of the Monte Carlo runs.

annual variability were identified in the meso- and eutrophic environments, while copepod variability in the oligotrophic environment was not characterized by a distinct seasonal mode (not reported here). In the oligotrophic environment, the first mode of cladoceran variability represents the entire summer stratified period, i.e., from the summer stratification onset until the time when the system becomes vertically homogeneous (June–November), and the second mode extends throughout the cold period of the year until the spring phytoplankton bloom (January–May). Aside from the “mirror effect” with regards to the loadings of the different months, the same seasonal modes also characterize the cladoceran patterns in the mesotrophic environment. Less clear was the cladoceran biomass variability in the eutrophic environment; the first sea-

sonal mode represents the entire cold period of the year as well as the spring bloom until the onset of summer stratification (December–June). The second mode corresponds to the run-to-run variability observed in July, September, and November, while May is almost equally loaded between the first and the second mode. The third mode is more strongly associated with the late-summer and mid-fall cladoceran variability (August and October).

The regression analysis aimed to identify the basic processes underlying the seasonal modes of cladoceran variability, using as predictor variables the zooplankton functional properties and the abiotic conditions examined in our Monte Carlo analysis. Aside from the second and third mode in the eutrophic environment, the multiple regression models

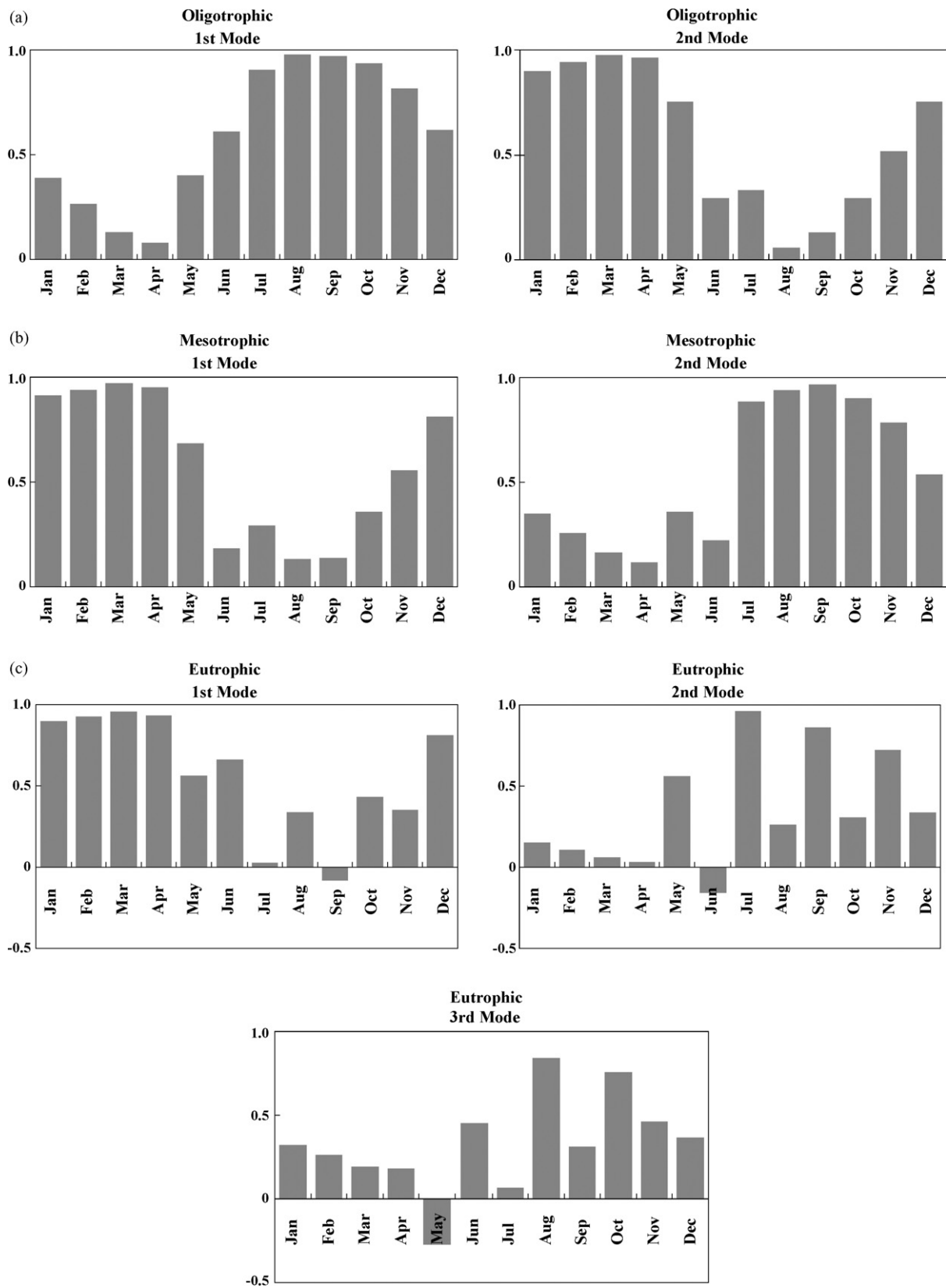


Fig. 3 – Rotated component coefficients for the principal components of cladoceran biomass across a trophic gradient ((a) oligotrophic; (b) mesotrophic; (c) eutrophic).

Table 3 – Multiple regression models developed for examining the most influential factors (plankton functional properties and abiotic conditions) associated with cladoceran biomass in three trophic states

First mode $r^2 = 0.932$		$ \beta $	Second mode $r^2 = 0.958$		$ \beta $			
Oligotrophic								
pred ₂		0.530	KTgr1 (CL) ^a		0.616			
T _{epi} ^a		0.465	T _{epi}		0.454			
pred ₁ ^a		0.348	T _{opt} (CL) ^a		0.395			
grazing _{max} (CL)		0.289	pred ₂		0.204			
Nutrient loading		0.252	grazing _{max} (CL)		0.195			
First mode $r^2 = 0.964$		$ \beta $	Second mode $r^2 = 0.933$		$ \beta $			
Mesotrophic								
KTgr1 (CL) ^a		0.631	pred ₁ ^a		0.501			
T _{epi}		0.464	pred ₂		0.497			
T _{opt} (CL) ^a		0.409	T _{epi} ^a		0.389			
pred ₂		0.243	grazing _{max} (CL)		0.347			
grazing _{max} (CL)		0.169	KZ (CL) ^a		0.223			
First mode $r^2 = 0.964$		$ \beta $	Second mode $r^2 = 0.571$		$ \beta $	Third mode $r^2 = 0.640$		$ \beta $
Eutrophic								
KTgr1 (CL) ^a	0.630	pred ₁ ^a	0.466	pred ₁ ^a	0.438			
T _{epi}	0.435	grazing _{max} (CO) ^a	0.316	grazing _{max} (CL)	0.422			
T _{opt} (CL) ^a	0.413	T _{epi} ^a	0.283	pred ₂	0.345			
pred ₂	0.272	bm _{ref} (CO)	0.171	grazing _{max} (CO)	0.234			
grazing _{max} (CO) ^a	0.252	KZ (CL) ^a	0.160	FQ _{Cyano}	0.208			

Symbol $|\beta|$ denotes the absolute value of the standardized coefficients.

^a Negative sign of the standardized coefficients.

explained over 90% of the between-run variability, and the five most significant predictors based on the absolute values of the standardized regression coefficients ($|\beta|$) are shown in Table 3. Representing the consumption from planktivorous fish, the specific zooplankton predation rate (pred₁) is negatively related to the summer cladoceran biomass with $|\beta|$ values higher than 0.350. The epilimnetic temperature (T_{epi}), the half saturation constant for predation (pred₂), and the maximum cladoceran grazing rate (grazing_{max} (CL)) are also significant predictors of cladoceran variability during the summer stratified period. A possible explanation for the negative T_{epi} effects ($|\beta| > 0.280$) on cladoceran biomass is the predominance of the temperature-dependent basal metabolism losses over animal growth in the summer epilimnetic environment. The half saturation constant for predation and maximum cladoceran grazing rate are both positively related to the cladoceran biomass with $|\beta|$ values approximately higher than 0.350 and 0.280, respectively. On the other hand, the half saturation constant for cladoceran grazing (KZ (CL)) has a (plausible) negative relationship with the cladoceran biomass in the meso- ($|\beta| = 0.223$) and eutrophic ($|\beta| = 0.160$) environment. The maximum grazing rate assigned to copepods (grazing_{max} (CO)) is also a significant predictor of the cladoceran variability in the eutrophic environment, but it is interesting to note that the negative effect manifested in the second mode (July, September, and November) switched to a positive one in the third mode of variability (August and October). Being modelled as a temperature-sensitive *Daphnia*-like species, the cladoceran variability is strongly associated with factors that determine the temperature effects on animal growth during the cold period of the year, such as the epilimnetic temperature T_{epi}

($|\beta| > 0.435$), the assigned optimal temperature for cladoceran growth T_{opt} (CL) ($|\beta| > 0.395$), and the sensitivity on water temperatures below the optimal one for growth KTgr1 (CL) ($|\beta| > 0.610$).

As previously mentioned, the PCA extracted two distinct modes of copepod variability in the meso- and eutrophic environments. The first seasonal mode corresponds to the period from May to December and is mainly driven by the effects of copepod basal metabolism rate (bm_{ref} (CO); $|\beta| > 0.355$) along with the maximum cladoceran (grazing_{max} (CL); $|\beta| > 0.372$) and copepod (grazing_{max} (CO); $|\beta| > 0.382$) grazing rates (Table 4). The copepod half saturation constant for grazing (KZ (CO)) plays a secondary role on the copepod variability with $|\beta|$ values within the 0.250–0.300 range. Interestingly, the competition between the two zooplankton functional groups becomes more evident in the eutrophic environment, where two parameters associated with the cladoceran feeding rates (i.e., grazing_{max} (CL) and KZ (CL)) are significant predictors of the copepod variability. The second seasonal mode covers the winter period until the time when the spring bloom peak usually occurs (January–April), and the most significant predictor of copepod variability is the predation from planktivorous fish (pred₁) with $|\beta|$ values higher than 0.425. We also highlight the positive relationship of the copepod biomass with KTgr1 (CL) ($|\beta| > 0.375$) or T_{opt} (CL) ($|\beta| > 0.250$), and the negative one with KTgr1 (CO) ($|\beta| \approx 0.290$); these factors reflect the importance of the assigned temperature requirements to attain optimal growth on the outcome of the competition between the two zooplankton functional groups. Finally, the monthly multiple regression models provide evidence that the copepod variability in the oligotrophic

Table 4 – Multiple regression models developed for examining the most influential factors (plankton functional properties and abiotic conditions) associated with copepod biomass in three trophic states

January $r^2 = 0.937$	$ \beta $	April $r^2 = 0.869$	$ \beta $	July $r^2 = 0.913$	$ \beta $	October $r^2 = 0.892$	$ \beta $
Oligotrophic							
grazing _{max} (CO)	0.443	KTgr1 (CL)	0.431	grazing _{max} (CO)	0.435	bm _{ref} (CO) ^a	0.506
bm _{ref} (CO) ^a	0.409	grazing _{max} (CO)	0.382	bm _{ref} (CO) ^a	0.388	grazing _{max} (CO)	0.399
pred ₁ ^a	0.311	pred ₁ ^a	0.339	grazing _{max} (CL) ^a	0.341	KZ (CO) ^a	0.311
KZ (CO) ^a	0.286	Nutrient loading	0.258	pred ₁ ^a	0.328	pred ₁ ^a	0.291
KTgr1 (CO) ^a	0.285	pred ₂	0.234	KZ (CO) ^a	0.272	pred ₂	0.271
First mode $r^2 = 0.834$		$ \beta $		Second mode $r^2 = 0.861$		$ \beta $	
Mesotrophic							
bm _{ref} (CO) ^a		0.415		pred ₁ ^a		0.425	
grazing _{max} (CO)		0.382		KTgr1 (CL)		0.404	
grazing _{max} (CL) ^a		0.372		KTgr1 (CO) ^a		0.299	
T _{epi} ^a		0.328		grazing _{max} (CO)		0.266	
KZ (CO) ^a		0.274		T _{opt} (CL)		0.258	
First mode $r^2 = 0.815$		$ \beta $		Second mode $r^2 = 0.879$		$ \beta $	
Eutrophic							
grazing _{max} (CL) ^a		0.468		pred ₁ ^a		0.553	
grazing _{max} (CO)		0.409		KTgr1 (CL)		0.375	
bm _{ref} (CO) ^a		0.355		KTgr1 (CO) ^a		0.289	
KZ (CL)		0.284		T _{opt} (CL)		0.277	
KZ (CO) ^a		0.253		grazing _{max} (CO)		0.246	

Principal component analysis (PCA) extracted two distinct modes of variability for the mesotrophic and eutrophic state. No distinct modes of variability were identified for the oligotrophic state; therefore, the multiple regression analysis was implemented individually on each month, and herein the results of four months (i.e., January, April, July, and October) are presented. Symbol $|\beta|$ denotes the absolute value of the standardized coefficients.

^a Negative sign of the standardized coefficients.

environment is mainly driven by their functional properties (i.e., grazing_{max} (CO), KZ (CO), bm_{ref} (CO)) and the planktivory control (pred₁), whereas evidence of the competition with cladocerans is only manifested in the summer stratified period, i.e., grazing_{max} (CL) with $|\beta| = 0.341$ in the July regression model.

3.3. Classification trees

We developed classification trees to gain further insight into the importance of the group-specific functional properties vis-à-vis the bottom-up effects (i.e., abiotic conditions and phytoplankton community) on the variability of the two zooplankton groups during the summer stratified period. The tree structures presented were cross-validated to avoid “overfitted” models, i.e., the classification tree computed from the learning sample (a randomly selected portion of the data sets) was used to predict class membership in the test sample (the remaining portion of the data sets) (Breiman et al., 1984; De'ath and Fabricius, 2000). In the tree analysis of the summer cladoceran biomass, the first split into two equally sized groups is identified when the total nitrogen (TN_{Jul}) concentration is 323.5 $\mu\text{g L}^{-1}$ (Fig. 4). When TN_{Jul} \leq 323.5 $\mu\text{g L}^{-1}$ the cladoceran biomass mainly varies between 35 and 70 $\mu\text{g C L}^{-1}$ (Class 2), whereas Class 3 (70–105 $\mu\text{g C L}^{-1}$) is dominant when TN_{Jul} $>$ 323.5 $\mu\text{g L}^{-1}$. A second critical total nitrogen concentration of 462.2 $\mu\text{g L}^{-1}$ further partitions the right branch of the tree (46% of the Monte Carlo runs) into two subbranches dominated by Class 3 (TN_{Jul} \leq 462.2 $\mu\text{g L}^{-1}$) and Class 5 cladoceran

biomass levels (TN_{Jul} $>$ 462.2 $\mu\text{g L}^{-1}$). Then, fish predation rates (pred₁) lower than 0.16 day⁻¹ result in cladoceran biomass levels within the Class 5 range (140–175 $\mu\text{g C L}^{-1}$). On the other hand, the left portion of the tree contains 54% of the Monte Carlo and the initial splitting condition is based on a phosphate (PO_{4Jul}) threshold of 2.8 $\mu\text{g L}^{-1}$. When this critical level is exceeded, the majority of cladoceran biomass concentrations fall within the range defined as Class 2 (35–70 $\mu\text{g C L}^{-1}$). Along the left branch, most cladoceran biomass values are subsequently partitioned based on critical phosphate (PO_{4Jul} = 4.4 $\mu\text{g L}^{-1}$) and total phosphorus (TP_{Jul} = 14.3 $\mu\text{g L}^{-1}$) concentrations, and eventually split into two terminal nodes where Class 3 (70–105 $\mu\text{g C L}^{-1}$) or Class 2 (35–70 $\mu\text{g C L}^{-1}$) dominate if the copepod biomass (CO_{Jul}) is lower or higher than the critical level of 33.2 $\mu\text{g C L}^{-1}$, respectively.

The initial splitting condition for copepod biomass is based on the cyanobacteria (CY_{Jul}) concentration, i.e., 37% of the total data set mainly dominated by Class 2 (35–70 $\mu\text{g C L}^{-1}$) biomass levels is classified on the right side of the tree when a cyanobacteria biomass threshold of 59.5 $\mu\text{g C L}^{-1}$ is exceeded (Fig. 5). Subsequently, copepod grazing rates (grazing_{max} (CO)) lower or higher than 0.46 day⁻¹ mainly result in Class 1 or Class 2 copepod biomass levels, respectively. Then, the exceedance of two thresholds of cyanobacteria values (84.0 and 79.6 $\mu\text{g C L}^{-1}$) is usually associated with higher copepod biomass. The left side of the tree, comprising 63% of the Monte Carlo runs, is mostly dominated by Class 1 (0–35 $\mu\text{g C L}^{-1}$) copepod concentrations. In this part of the tree, the two main splitting conditions are related to the ambient phosphate lev-

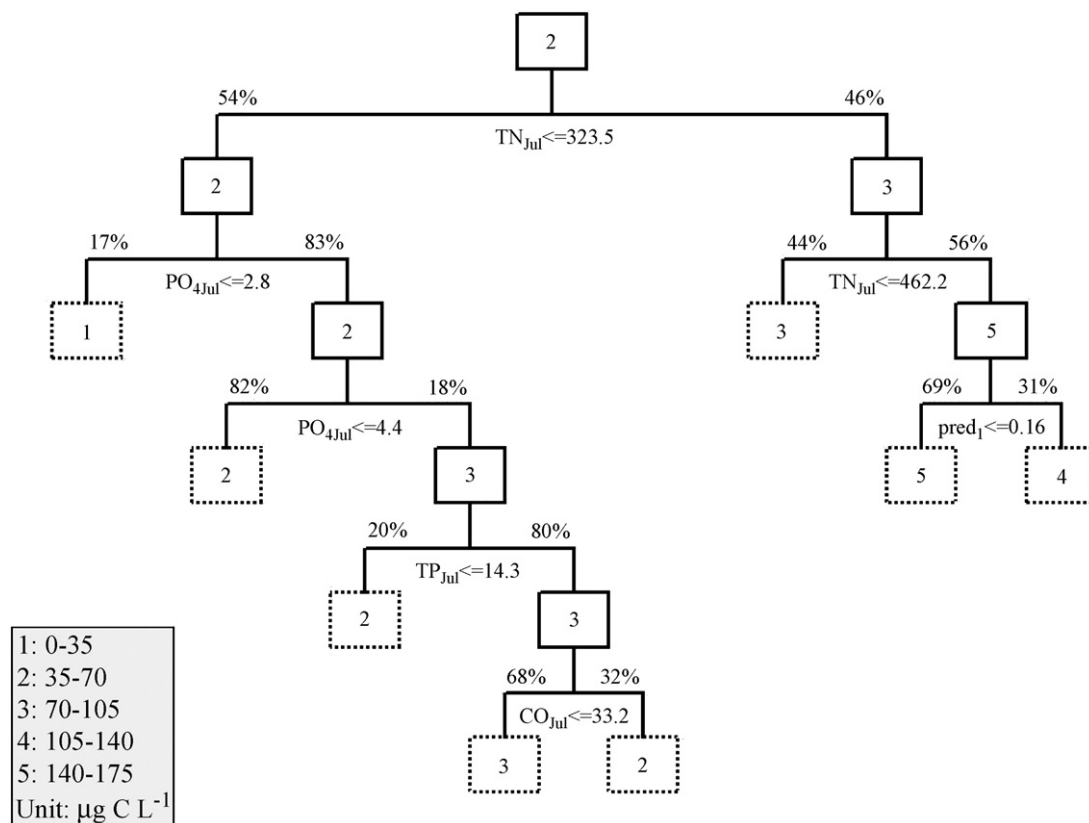


Fig. 4 – Classification tree diagram of cladoceran biomass under nutrient enrichment conditions. Dependent variable is the cladoceran biomass in July; predictors include all cladoceran functional properties and the abiotic conditions along with the major limnological variables in July. Solid and dashed boxes represent the split and terminal nodes, respectively. The cases of the parent nodes are sent to the left child nodes if the corresponding values are no greater than the split conditions; otherwise they are sent to the right child nodes. The numbers in the boxes represent the dominant categorical value of cladoceran biomass. The percentage values represent the percent of learning sample from parent nodes going to the corresponding child nodes. The cross-validation cost for this classification tree is 31.7%.

els ($\text{PO}_{4\text{Jul}} = 6.4 \mu\text{g L}^{-1}$) and the maximum copepod grazing rate ($\text{grazing}_{\text{max}}(\text{CO}) \leq 0.48 \text{ day}^{-1}$). The remaining data are separated into two terminal nodes dominated by Class 1 and Class 2 concentrations, based on a cyanobacteria biomass threshold of $51.1 \mu\text{g C L}^{-1}$. Other influential factors of the copepod variability were the dissolved inorganic (DIN_{Jul}) and total nitrogen (TN_{Jul}) concentrations along with the copepod basal metabolism rate ($\text{bm}_{\text{ref}}(\text{CO})$). Finally, it should be noted that the cross-validation cost (i.e., an estimate of the misclassification error) for the two classification trees was 31.7 and 18.1%, respectively.

3.4. Examination of the role of selected parameters under nutrient enrichment conditions

We further examined the effects of the cyanobacteria food quality ($\text{FQ}(\text{CY})$), the critical threshold for mineral P limitation (C:P_0), and the half saturation constant for growth efficiency (ef_2) on the zooplankton functional group biomass across a range of nutrient loading. Maintaining all the rest forcing functions at reference values (Arhonditsis and Brett, 2005b), a series of nutrient loadings was created spanning the 10–300% range of the reference exogenous nutrient input

(0.58–17.4 mg TOC/L, 97–2901 $\mu\text{g TN/L}$, 6.5–195 $\mu\text{g TP/L}$), with an increment of 10%. For each nutrient loading, the model was run for a ten-year period, which was a sufficient simulation period to reach “equilibrium” phase; i.e., the same pattern was repeated each year. The zooplankton biomass was recorded subsequently at an arbitrarily chosen day in the summer (15 July) of the tenth year. Thereafter, we started a simulation in which one model parameter of interest (e.g., $\text{FQ}(\text{CY})$) was changed, and all the other parameters were kept as in the calibration vector reported in the Lake Washington presentation (Arhonditsis and Brett, 2005a). We also examined a second loading scenario in which total phosphorus inflows were varied within the 10–300% range, while the total organic carbon and nitrogen inputs were kept at the current levels in Lake Washington.

The effects of cyanobacteria food quality ($\text{FQ}(\text{CY})$) and half saturation constant for zooplankton growth efficiency (ef_2) on zooplankton group biomass under nutrient enrichment conditions are shown in Fig. 6. In the first loading scenario, both cladoceran and copepod biomass show monotonic increase with the total phosphorus concentrations, whereas the second enrichment scenario is characterized by zooplankton biomass–total phosphorus relationship with a

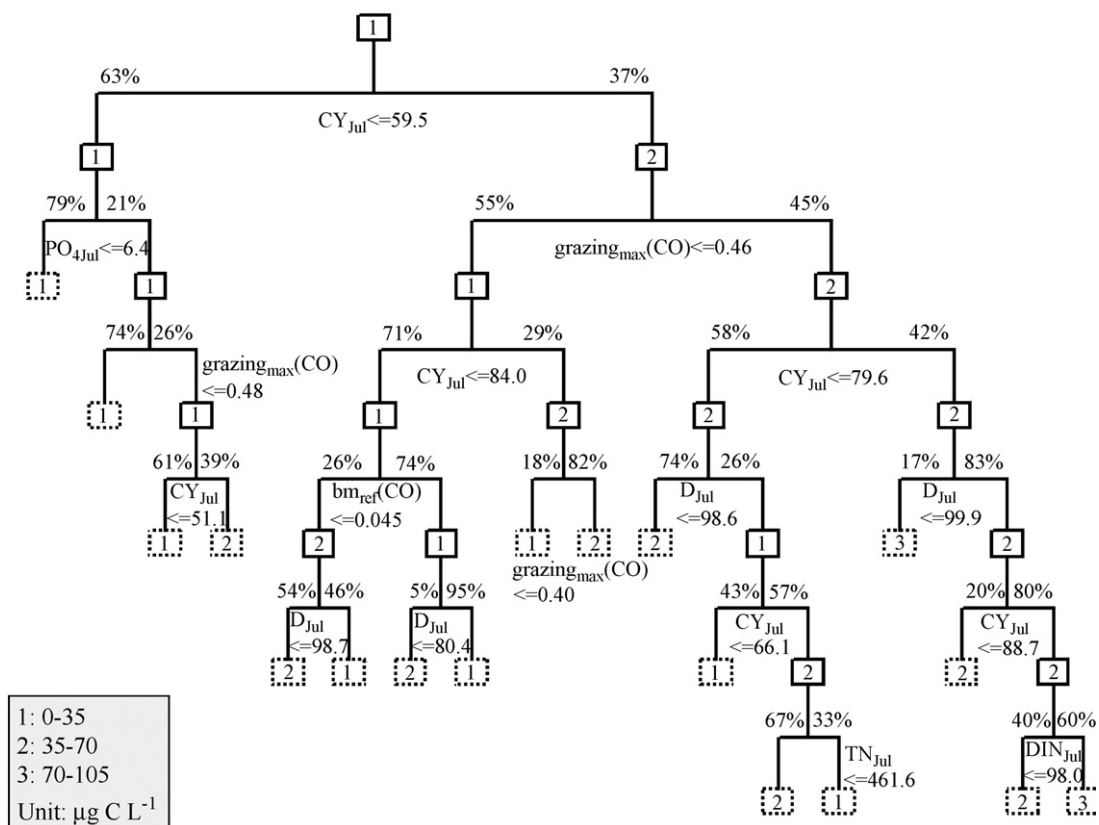


Fig. 5 – Classification tree diagram of copepod biomass under nutrient enrichment conditions. Dependent variable is the copepod biomass in July; predictors include all copepod functional properties and the abiotic conditions along with the major limnological variables in July. The cross-validation cost for this classification tree is 18.1%.

concave (concave-down) shape where the apex (maximum extremum) is usually located around the 20–25 $\mu\text{g TPL}^{-1}$ level. The subregion where zooplankton biomass decreases with increasing total phosphorus concentrations probably stems from the low detritus (POC) levels along with the structural shifts of the phytoplankton community induced from the prevalence of nitrogen-limiting conditions (see next paragraph). The biomass of the two zooplankton functional groups has an increasing trend with respect to FQ(CY) along the nutrient loading range. [It should be noted that the negative FQ(CY) values represent the potential impact of mechanical interference by filamentous cyanobacteria (e.g., *Oscillatoria rubescens*) on zooplankton feeding.] On the other hand, the zooplankton biomass-half saturation constant for zooplankton growth efficiency (ef_2) relationship is monotonically decreasing throughout the total phosphorus concentrations. We also examined the effects of the critical threshold for mineral P limitation ($C:P_0$) on the cladoceran biomass using a range that starts from 35 (i.e., the cladoceran somatic ratio) to 145 (Fig. 7). The cladoceran biomass exhibits an increasing trend with respect to $C:P_0$ until a maximum value is reached, usually located within the 65–95 range, and thereafter the cladoceran biomass remains constant.

We finally plotted the three phytoplankton group biomass against the two zooplankton functional groups (Fig. 8). Under the first nutrient enrichment scenario, the phytoplankton-zooplankton relationships have a positive

slope until a global maximum is reached (150–200% of the reference nutrient loading conditions), then the net phytoplankton growth rate is negative and their biomass declines. Both diatoms and green algae follow a similar trajectory across the phosphorus loading gradient. In contrast, cyanobacteria gain competitive advantage and dominate the phytoplankton community at the hypereutrophic state. In the latter case, the biomass of the two zooplankton functional groups also declines in response to the qualitative and quantitative changes in the phytoplankton community.

4. Discussion

Being one of the most poorly modelled components of the aquatic food webs, zooplankton dynamics are often highlighted as a main area of where deeper understanding and more articulate mathematical representation of the underlying processes should be sought (Franks, 2002; Arhonditsis and Brett, 2004; Flynn, 2005; Mitra et al., 2007). The improvement in zooplankton modelling requires reliable and robust parameterization of a number of processes, such as ingestion (prey selectivity and grazing strategies); digestion (extraction of material from the ingested prey), assimilation of the material into predator biomass; metabolic rates (respiration, excretion, mortality); and planktivory. Zooplankton growth is driven by the complex interplay among these processes and is fur-

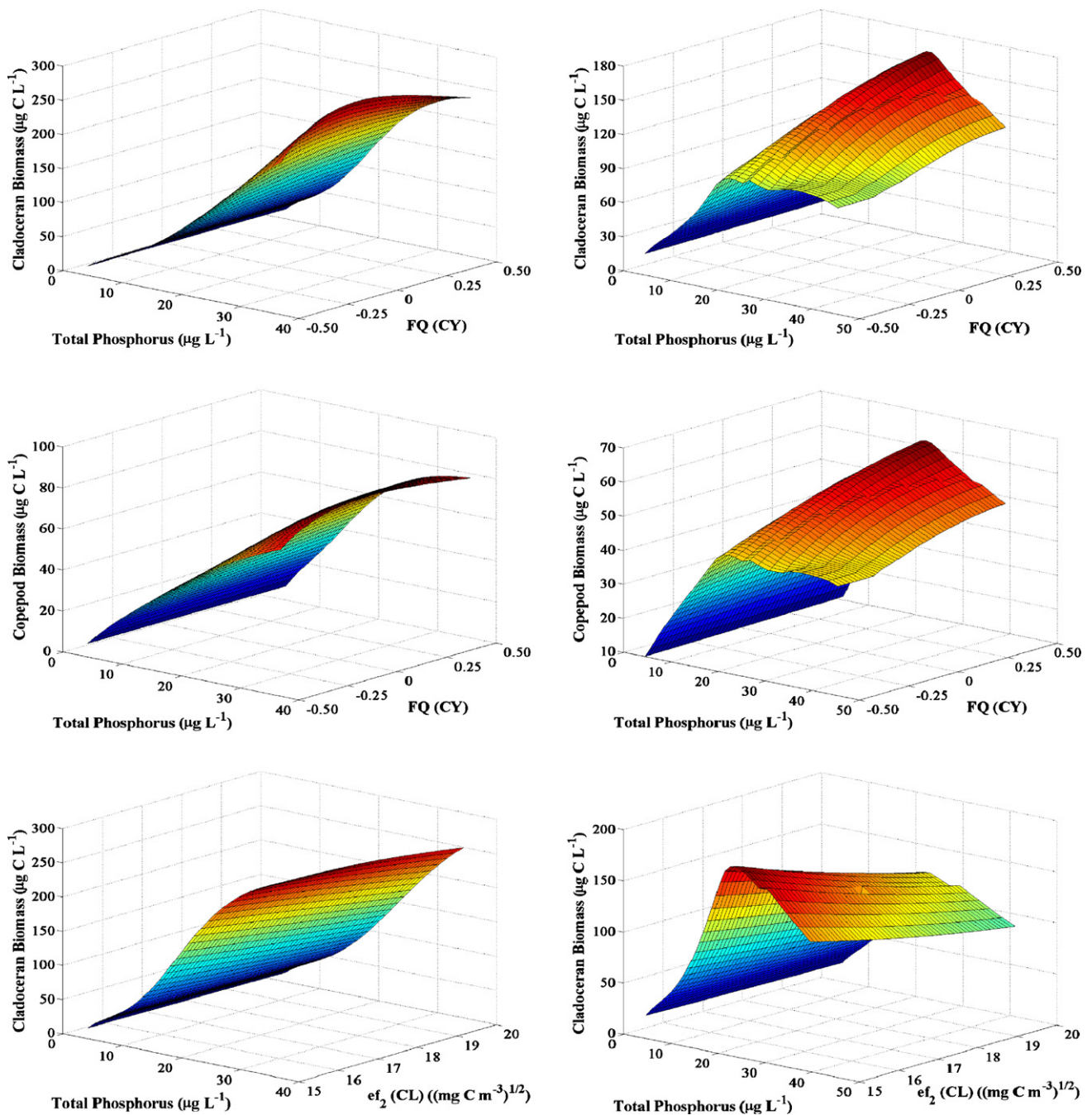


Fig. 6 – Effects of the cyanobacteria food quality and the half saturation constant for growth efficiency on the zooplankton functional group biomass across a range of nutrient loading that corresponds to the 10–300% of the current total organic carbon, total nitrogen, and total phosphorus loading in Lake Washington (left panel). The right panel plots correspond to a similar variation of the total phosphorus inflows, while the total carbon and nitrogen inputs were kept to the present level.

ther modulated from biochemical factors (lipids, fatty acids) along with the stoichiometric disparities between predator and prey that control the efficiency and the rates at which phytoplankton standing stock is converted to herbivore biomass (Sterner and Hessen, 1994; Brett and Muller-Navarra, 1997; Elser and Urabe, 1999). By acknowledging the idiosyncrasies and behavioural complexities of the zooplankton ecology, we believe that the development of complex models, founded upon a critical synthesis of existing knowledge, can provide

excellent heuristic tools for enhancing our understanding of plankton dynamics. In this regard, we present a probabilistic analysis of the input vector of a complex aquatic biogeochemical model that offers insights into the relative role of the zooplankton functional properties (e.g., feeding strategies, food quality, predation rates, stoichiometry, basal metabolism, and temperature requirements) and the abiotic conditions (temperature, nutrient loading) on competition patterns and structural shifts in plankton communities.

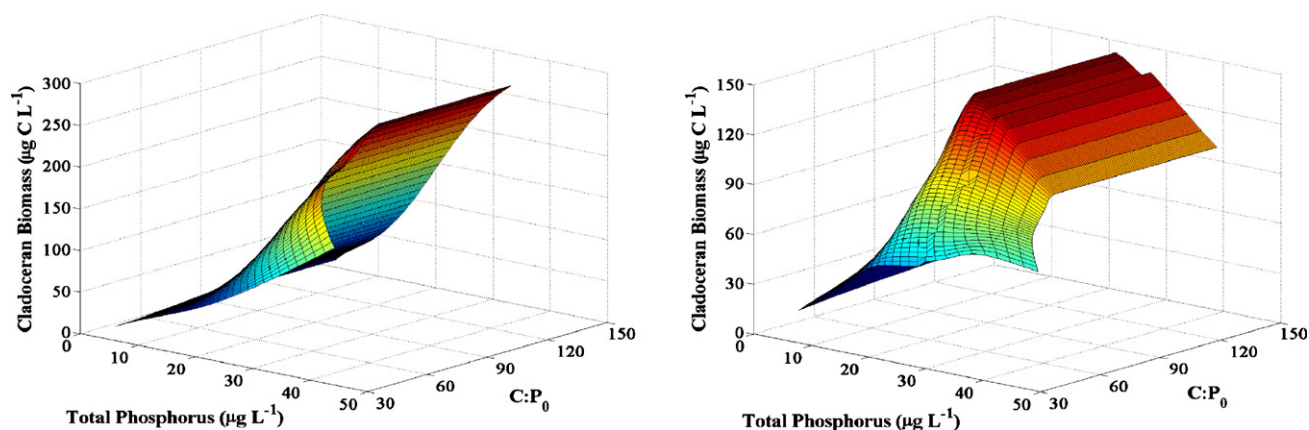


Fig. 7 – Effects of the critical threshold for mineral P limitation ($C:P_0$) on the cladoceran biomass across a range of nutrient loading that corresponds to the 10–300% of the current total organic carbon, total nitrogen, and total phosphorus input concentrations in Lake Washington (left panel). The right panel plots correspond to a similar variation of the total phosphorus inflows, while the total carbon and nitrogen input were kept to the present level.

The straightforward delineation of the modelled zooplankton groups (i.e., cladocerans, copepods) along with their distinct functional properties resulted in an accurate reproduction of the seasonal succession plankton patterns usually observed in temperate thermally stratified lakes (Lampert and Sommer, 1997; Wetzel, 2001). The annual copepod cycle in meso- and eutrophic environments was split into two independent seasonal modes that together accounted for more than 87% of the between-run variability observed in our numerical experiments. Being designed as a *Diaptomus*-like species, copepods are assigned wider temperature tolerance and higher feeding rates ($KZ(CO) < KZ(CL)$) at low food levels that allow dominating the overwintering zooplankton community. The same competitive advantages can also explain their prompt response to the initiation of the spring phytoplankton bloom when the maximum copepod abundance (median values of $70\text{--}120\ \mu\text{g C L}^{-1}$) is usually reached at the end of April (Fig. 2). During this period (January–April), the main drivers of the copepod variability are the relative differences between the copepod and cladoceran temperature requirements to attain optimal growth along with the control exerted from planktivorous fish. On the other hand, the winter cladoceran biomass is relatively low representing the usual development of resting stages (e.g., diapausing ephippia in the sediments), and the temperature limitation is gradually relaxed after the end of May ($T_{\text{epi}} \geq 10^\circ\text{C}$). Soon thereafter, the cladocerans become the dominant group of the summer zooplankton community, when their run-to-run variability is mainly associated with the temperature-dependent growth minus basal metabolism loss balance along with consumption rates from planktivorous fish. The *Daphnia*-like species is the dominant group of the zooplankton community until the prevailing winter conditions (e.g., low temperatures and low food availability) become unfavourable for its growth, whereas the copepods are well adapted for the winter habitat and gain competitive advantage.

Interestingly, the cladoceran variability is split into two distinct modes during the stratified period in the eutrophic environment. This pattern arises from the (approximately)

two-month period prey–predator oscillations manifested in response to the increased nutrient loading (Fig. 2). The emergence of increased oscillatory behaviour in the system is then followed by gradual biomass decrease of one (Fig. 8, left panel) or both (Fig. 8, right panel) of the two trophic levels modelled. Namely, our numerical experiments provide evidence of potentially destabilizing effects on the system under increasing nutrient loading conditions. Plausible mechanisms associated with these system destabilization patterns can be drawn from the significant predictors of the pertinent regression model along with the theories proposed to resolve Rosenzweig’s enrichment paradox (Roy and Chattopadhyay, 2007). The significantly positive regression coefficient of the cyanobacteria food quality on the third mode of cladoceran variability highlights the importance of the unpalatable prey, i.e., a prey that is edible but its quality does not meet the nutritional requirements of the predator populations. Genkai-Kato and Yamamura (1999, 2000) showed that the presence of an unpalatable prey in enriched systems increases the robustness of stability of the predator–prey systems by reducing the amplitude of oscillations and/or by preventing species from falling below critical abundance levels. Hence, as the increasing nutrient loading relaxes the phosphorus limitation favouring cyanobacteria dominance in the system, the food quality assigned to our cyanobacteria-like species modulates the amplitude of the prey–predator oscillations and becomes an influential factor of the cladoceran variability during the stratified period.

We also emphasize the significant role of the higher predation terms parameterized as being dependent on the zooplankton density, i.e., our cladoceran closure term assumes a “switchable” type of predation from planktivorous fish, while the higher predation on copepods is represented by a hyperbolic form. In the context of nutrient enrichment, Gatto (1991) showed that the introduction of a density-dependent mortality term in a simple predator–prey model could stabilize prey–predator dynamics. Likewise, we found that the control exerted from the planktivores is a significant driver of the zooplankton variability throughout the annual cycle

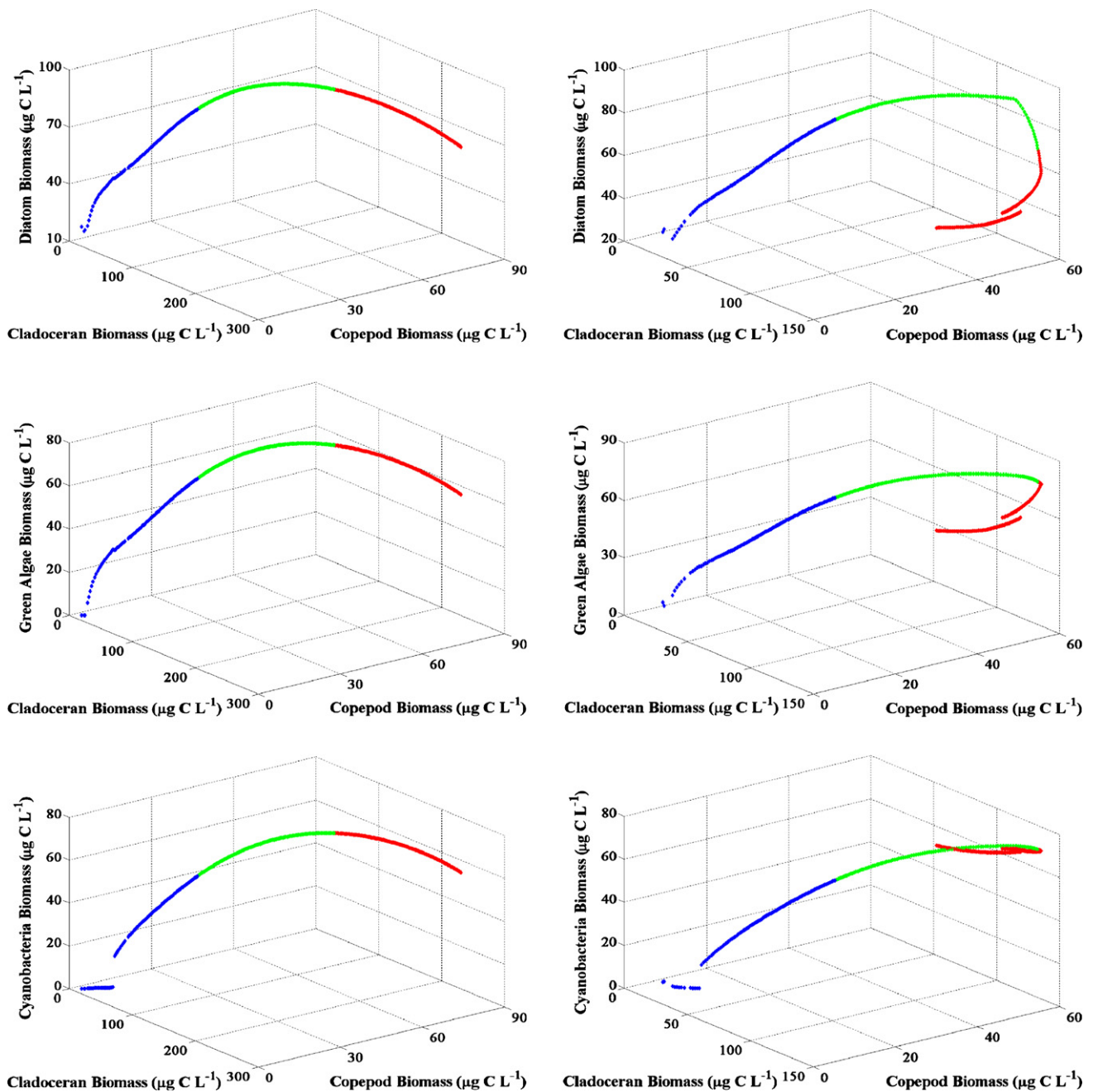


Fig. 8 – State-space for the two zooplankton functional group biomass versus the three phytoplankton functional group biomass across a wide range of total nutrient (left panel) and phosphorus (right panel) loading. Blue, green, and red portions correspond to loading ranges of 1–100, 100–200, and 200–300% of the present loading in Lake Washington, respectively. (For interpretation of the references to colour in this figure legend, the reader is referred to the web version of the article.)

underscoring its importance for the dynamics produced from plankton ecosystem models (Edwards and Yool, 2000). Generally, at a given nutrient availability, Danielsdottir et al. (2007) indicated that the interplay between food quality and zooplanktivory determines the zooplankton biomass, i.e., when phytoplankton food quality is high the zooplankton can withstand intense zooplanktivory, whereas when food quality is low zooplankton can easily be eliminated. Finally, we note the counterintuitive positive sign of the regression coefficient relating cladoceran variability to the maximum copepod graz-

ing rate during the third mode. This positive relationship probably implies that the increase in the grazing strength of the second predator (copepods) in the eutrophic environment can pave the way (e.g., increase of the detritus pool from the egested biogenic material) for the dominant grazer (cladocerans), thereby inducing higher amplitude oscillations.

The classification tree analysis suggests that under nutrient enrichment conditions the summer copepod biomass increase is closely associated with the exceedance of several threshold levels of cyanobacteria abundance. Copepods

are modelled as being capable of selecting their food on the basis of its nutritional quality, but this selectivity changes dynamically as a function of the relative proportion of the four food-types (DeMott, 1989; Fasham et al., 1990). Although the feeding behavioural adaptability of copepods in lakes with significant populations of cyanobacteria has been discussed in the literature (Vanderploeg et al., 1990; DeMott and Moxter, 1991), the question arising here is how possible is to find such close connection between cyanobacteria and copepods in real world conditions? The ability of the copepods to exhibit high clearance rates on cyanobacteria filaments/colonies and to avoid toxic strains does not rule out a positive relationship (DeMott and Moxter, 1991). However, given the excellent copepod selectivity in habitats with high concentration-mixtures (Vanderploeg et al., 1988; DeMott, 1988, 1989; DeMott and Moxter, 1991), it is unlikely that this relationship can be manifested in a system where cyanobacteria account for less than 30% of the total phytoplankton abundance. In the mesotrophic environment, this parameterization resulted in a copepod diet consisting of 80–85% of diatoms and detritus, 20% of green algae, and less than 5–10% of cyanobacteria during the summer stratified period. As we move further along the nutrient loading gradient, the cyanobacteria proportion to the total phytoplankton biomass increases ($\approx 30\%$), but because of the copepod ability to distinguish and actively ingest favourable food the relative contribution of the different food-types to their diet does not change significantly. Therefore, the results of the classification tree analysis are not an indication of a strong causal link between the two groups. They probably stem from the concurrent cyanobacteria and copepod increase which, however, is driven by different changes of the system functioning under the nutrient enrichment conditions, i.e., a relaxation of the phosphorus limitation for cyanobacteria and an increase of the availability of the desirable food-types for copepods.

In a similar manner, the tree analysis of the summer cladoceran biomass identified two major splitting conditions for which there was no apparent causal connection, i.e., the exceedance of two critical total nitrogen concentrations was associated with higher cladoceran abundance. This result is probably related to the assumption of zooplankton's ability to maintain its somatic elemental (C:N:P) ratios constant by independently adjusting the production efficiency (biomass produced per food ingested) for carbon, nitrogen, and phosphorus, which results in an increased model sensitivity to the non-limiting elemental (carbon and nitrogen) recycling (Arhonditsis and Brett, 2005b). In particular, the stoichiometric theory predicts that zooplankton with low body C:P and N:P ratios recycle nutrients at higher C:P and N:P ratios than zooplankton taxa with high somatic C:P and N:P ratios (Elser and Urabe, 1999). Based on this proposition, the P-rich animals (e.g., *Daphnia*) should contribute a significant proportion of the excess carbon and nitrogen being recycled in the system. This direct link between TN-cladoceran abundance is manifested in the tree diagram, although in a strict causal sense the relationship exists in reverse direction. Yet, recent empirical and modelling studies provide evidence that the assumption of strict element homeostasis does not always explain *Daphnia* dynamics in P-deficient environments (Mulder and Bowden, 2007; Ferrao-Filho et al., 2007). The relaxation of this

assumption with the inclusion of a variable nutrient assimilation and nutrient use efficiency from zooplankton should test the robustness of the tight connection between the levels of the non-limiting elements and the cladoceran biomass. A second assumption of our model that invites further examination involves the fate of the excess non-limiting nutrients in the system. Arhonditsis and Brett (2005b) found that the assignment of a higher value to the particulate fraction of the egested material more closely reproduces the observed Lake Washington patterns. This partitioning renders support to the hypothesis that zooplankton homeostasis is maintained during the digestion and assimilation process, i.e., by removing elements in closer proportion to zooplankton body ratios than to the elemental ratio of the food (Elser and Foster, 1998). By contrast, Anderson et al. (2005) using a model with an explicit representation of the consumer metabolic processes supported the hypothesis that multi-nutrient balancing is regulated by post-absorptive mechanisms, i.e., homeostasis is maintained via post-assimilation processing and differential excretion of nutrients in dissolved form.

Driven from the formulation used to describe the phosphorus production efficiency, our numerical experiments suggest that food availability places the greatest limitation on zooplankton growth in oligotrophic systems. At the lower end of the two enrichment scenarios, the zooplankton response was primarily related to the phytoplankton increase, regardless of the food quality assigned to cyanobacteria or the half saturation constant for assimilation efficiency (Fig. 6), the critical C:P₀ ratio above which zooplankton experiences mineral P limitation (Fig. 7), and the composition of the phytoplankton community (Fig. 8). Based on data from 33 different sources, a recent empirical modelling study from Persson et al. (2007) showed qualitatively similar zooplankton limitation patterns, i.e., food quantity imposes the greatest limitations on *Daphnia* growth in nutrient poor lakes ($TP \leq 4 \mu\text{g L}^{-1}$). The same study also predicted an increased phosphorus limitation on *Daphnia* growth with decreasing TP, whereas the biochemical quality imposed food quality constraints over the entire trophic gradient examined and was particularly important in the most productive lakes (Persson et al., 2007). Our dynamic parameterization places somewhat greater weight on the role of food abundance, as the effects of food quality are not manifested until the summer TP concentrations exceed an approximate level of 10–12 $\mu\text{g L}^{-1}$. Thereafter, both biochemical quality and phosphorus availability come into play and regulate the energy transfer at the plant–animal interface. In particular, when the enrichment conditions alleviate phosphorus limitation thereby promoting cyanobacteria dominance (second loading scenario), food quality appears to be closely related to the herbivore biomass variability. Cyanobacteria-dominated phytoplankton communities are characterized by low $\omega 3$ -polyunsaturated fatty acids ($\omega 3$ -PUFAs), e.g., eicosapentaenoic acid (EPA), docosahexaenoic acid (DHA) and octadecatetraenoic acid, which are very important for zooplankton growth and egg-production (Brett and Muller-Navarra, 1997; Muller-Navarra et al., 2004). The ramifications for the zooplankton community from such undesirable shifts in the phytoplankton community structure are dependent on the availability of alternative food sources in the system, e.g., the differences between the two enrich-

ment scenarios in Fig. 8 reflect the role of detritus modelled as an intermediate quality food-type (Arhonditsis and Brett, 2005a). On the other hand, the seston C:P values in the three trophic environments were consistently lower than the critical threshold (C:P₀) ratios (87–145 mgC mgP⁻¹) proposed as limiting for zooplankton growth (Brett et al., 2000), whereas the direct impact of P-limitation is unlikely to be experienced in the 36–85 (weight ratio) range examined in Fig. 7. Generally, the effects of mineral P-limitation on various aspects of zooplankton growth seem to be more strongly supported in the literature (Sterner and Hessen, 1994; Gulati and DeMott, 1997; Sterner and Elser, 2002), although Persson et al. (2007) pointed out that the majority of this research focused on extremely high seston C:P ratios representing only a small portion of lakes with very low TP concentrations. Finally, it should be noted that one aspect not explicitly considered in this analysis involves the indirect effects of the nutrient-stressed cells on zooplankton growth, e.g., morphological cell changes that reduce their digestibility (Van Donk et al., 1997; Ravet and Brett, 2006).

In conclusion, we used a complex aquatic biogeochemical model to examine competition patterns and structural shifts in the plankton community across a trophic gradient. Our analysis indicated that the group-specific maximum grazing rates, the predation rates from planktivorous fish, along with the temperature requirements to attain optimal growth could be particularly influential on the seasonal succession patterns of plankton communities. Our numerical experiments provide evidence that food availability is a major regulatory factor of the zooplankton growth in oligo- and mesotrophic systems. We also highlight the dire effects that the cyanobacteria food quality can have on the zooplankton community in productive systems, where the biomass levels of the different zooplankton functional groups are related to the availability of alternative food sources, e.g., diatoms, detritus, green algae. The control exerted from the planktivores is another significant factor for system stability under increasing nutrient loading conditions. Food quality and zooplanktivory interact to determine zooplankton dynamics and combinations of low food quality and high fish predation can cause zooplankton elimination. The mathematical representation of the producer–grazer interactions in stoichiometrically and/or biochemically realistic terms in ecosystem models is necessary, as it offers insights into the patterns of nutrient and energy flow transferred to the higher trophic levels. While there are sound arguments against using complex mathematical models, we believe that there are equally important reasons to avoid oversimplified model structures that may directly or indirectly obfuscate the role of important ecological processes on ecosystem functioning.

Acknowledgements

Funding for this study was provided by the UTSC Research Fellowships (Master of Environmental Science Program, Centre for Environment & University of Toronto at Scarborough) and the Connaught Committee (University of Toronto, Matching Grants 2006–2007).

REFERENCES

- Andersen, T., 1997. Pelagic Nutrient Cycles: Herbivores as Sources and Sinks. Springer-Verlag, New York, NY, USA, 280 pp.
- Anderson, T.R., Hessen, D.O., Elser, J.J., Urabe, J., 2005. Metabolic stoichiometry and the fate of excess carbon and nutrients in consumers. *Am. Nat.* 165, 1–15.
- Arhonditsis, G.B., Brett, M.T., 2004. Evaluation of the current state of mechanistic aquatic biogeochemical modelling. *Mar. Ecol. Prog. Ser.* 271, 13–26.
- Arhonditsis, G.B., Brett, M.T., 2005a. Eutrophication model for Lake Washington (USA). Part I. Model description and sensitivity analysis. *Ecol. Model.* 187, 140–178.
- Arhonditsis, G.B., Brett, M.T., 2005b. Eutrophication model for Lake Washington (USA). Part II. Model calibration and system dynamics analysis. *Ecol. Model.* 187, 179–200.
- Arhonditsis, G.B., Tsirtsis, G., Karydis, M., 2000. Quantification of the effects of non-point sources to coastal marine eutrophication: applications to a semi-enclosed gulf in the Mediterranean Sea. *Ecol. Model.* 129, 209–227.
- Arhonditsis, G.B., Winder, M., Brett, M.T., Schindler, D.E., 2004. Patterns and mechanisms of phytoplankton variability in Lake Washington (USA). *Water Res.* 38, 4013–4027.
- Breiman, L., Friedman, J.H., Olshen, R.A., Stone, C.J., 1984. Classification and Regression Trees. Wadsworth International Group, Belmont, CA, USA, 358 pp.
- Brett, M.T., Goldman, C.R., 1997. Consumer versus resource control in freshwater pelagic food webs. *Science* 275, 384–386.
- Brett, M.T., Muller-Navarra, D.C., 1997. The role of highly unsaturated fatty acids in aquatic foodweb processes. *Freshwater Biol.* 38, 483–499.
- Brett, M.T., Muller-Navarra, D.C., Park, S.K., 2000. Empirical analysis of mineral P limitation's impact on algal food quality for freshwater zooplankton. *Limnol. Oceanogr.* 47, 1564–1575.
- Brett, M.T., Arhonditsis, G.B., Mueller, S.E., Hartley, D.M., Frodge, J.D., Funke, D.E., 2005. Non-point-source impacts on stream nutrient concentrations along a forest to urban gradient. *Environ. Manage.* 35, 330–342.
- Broekhuizen, N., Heath, M.R., Hay, S.J., Gurney, W.S.C., 1995. Modelling the dynamics of the North Sea's mesozooplankton. *Netherlands J. Sea Res.* 33, 381–406.
- Chen, C., Ji, R., Schwab, D.J., Beletsky, D., Fahnenstiel, G.L., Jiang, M., Johengen, T.H., Vanderploeg, H., Eadie, B., Budd, J.W., Bundy, M.H., Gardner, W., Cotner, J., Lavrentyev, P.J., 2002. A model study of the coupled biological and physical dynamics in Lake Michigan. *Ecol. Model.* 152, 145–168.
- Danielsdottir, M.G., Brett, M.T., Arhonditsis, G.B., 2007. Phytoplankton food quality control of planktonic food web processes. *Hydrobiologia* 589, 29–41.
- De'ath, G., Fabricius, K.E., 2000. Classification and regression trees: a powerful yet simple technique for ecological data analysis. *Ecology* 81, 3178–3192.
- DeMott, W.R., 1988. Discrimination between algal and artificial particles by freshwater and marine copepods. *Limnol. Oceanogr.* 33, 397–408.
- DeMott, W.R., 1989. Optimal foraging theory as a predictor of chemically mediated food selection by suspension-feeding copepods. *Limnol. Oceanogr.* 34, 140–154.
- DeMott, W.R., Moxter, F., 1991. Foraging on cyanobacteria by copepods—responses to chemical defenses and resource abundance. *Ecology* 72, 1820–1834.
- Doney, S.C., Glover, D.M., Najjar, R.G., 1996. A new coupled, one-dimensional biological-physical model for the upper ocean: applications to the JGOFS Bermuda Atlantic time-series study (BATS) site. *Deep-Sea Res. II* 43, 591–624.

- Downing, J.A., Rigler, F.H., 1984. A Manual on Methods for the Assessment of Second Productivity in Fresh Water, second ed. Blackwell Scientific Publications, Oxford, UK, 501 pp.
- Ederington, M.C., McManus, G.B., Harvey, H.R., 1995. Trophic transfer of fatty-acids, sterols and a triterpenoid alcohol between bacteria, a ciliate and the copepod *Acartia tonsa*. *Limnol. Oceanogr.* 40, 860–867.
- Edwards, A.M., Yool, A., 2000. The role of higher predation in plankton population models. *J. Plankton Res.* 22, 1085–1112.
- Elser, J.J., Foster, D.K., 1998. N:P stoichiometry of sedimentation in lakes of the Canadian shield: relationships with seston and zooplankton elemental composition. *Ecoscience* 5, 56–63.
- Elser, J.J., Urabe, J., 1999. The stoichiometry of consumer-driven nutrient recycling: theory, observations, and consequences. *Ecology* 80, 735–751.
- Fasham, M.J.R., 1993. Modelling the marine biota. In: Heimann, M. (Ed.), *The Global Carbon Cycle*. Springer-Verlag, Berlin, Germany, pp. 457–504.
- Fasham, M.J.R., Ducklow, H.W., McKelvie, S.M., 1990. A nitrogen-based model of plankton dynamics in the oceanic mixed layer. *J. Mar. Res.* 48, 591–639.
- Fennel, W., 2001. Modelling of copepods with links to circulation models. *J. Plankton Res.* 23, 1217–1232.
- Fennel, W., Neumann, T., 2001. Coupling biology and oceanography in models. *Ambio* 30, 232–236.
- Ferrao-Filho, A.D., Tessier, A.J., DeMott, W.R., 2007. Sensitivity of herbivorous zooplankton to phosphorus-deficient diets: testing stoichiometric theory and the growth rate hypothesis. *Limnol. Oceanogr.* 52, 407–415.
- Flynn, K.J., 2005. Castles built on sand: dysfunctionality in plankton models and the inadequacy of dialogue between biologists and modellers. *J. Plankton Res.* 27, 1205–1210.
- Franks, P.J.S., 2002. NPZ models of plankton dynamics: their construction, coupling to physics, and application. *J. Oceanogr.* 58, 379–387.
- Franks, P.J.S., Chen, C.S., 2001. A 3-D prognostic numerical model study of the Georges bank ecosystem. Part II. Biological–physical model. *Deep-Sea Res. II* 48, 457–482.
- Gatto, M., 1991. Some remarks on models of plankton densities in lakes. *Am. Nat.* 137, 264–267.
- Genkai-Kato, M., Yamamura, N., 1999. Unpalatable prey resolves the paradox of enrichment. *Proc. R. Soc. Lond. B—Biol. Sci.* 266, 1215–1219.
- Genkai-Kato, M., Yamamura, N., 2000. Profitability of prey determines the response of population abundances to enrichment. *Proc. R. Soc. Lond. B—Biol. Sci.* 267, 2397–2401.
- Grover, J.P., 1997. *Resource Competition*. Chapman and Hall, London, UK, 342 pp.
- Gulati, R.D., DeMott, W.R., 1997. The role of food quality for zooplankton: remarks on the state-of-the-art, perspectives and priorities. *Freshwater Biol.* 38, 753–768.
- Hessen, D.O., Andersen, T., 1992. The algae-grazer interface: feedback mechanisms linked to elemental ratios and nutrient cycling. *Arch. Hydrobiol. Beih. Ergebn. Limnol.* 35, 111–120.
- Hessen, D.O., Lyche, A., 1991. Interspecific and intraspecific variations in zooplankton element composition. *Arch. Hydrobiol.* 121, 343–353.
- Jassby, A.D., 1999. Uncovering mechanisms of interannual variability from short ecological time series. In: Scow, K.M., Fogg, G.E., Hinton, D.E., Johnson, M.L. (Eds.), *Integrated Assessment of Ecosystem Health*. CRC Press, Boca Raton, FL, USA, pp. 285–306.
- Jorgensen, S.E., Bendoricchio, G., 2001. *Fundamentals of Ecological Modelling*, third ed. Elsevier, Amsterdam, The Netherlands, 530 pp.
- Jorgensen, S.E., Nielsen, S.N., Jorgensen, L.A., 1991. *Handbook of Ecological Parameters and Ecotoxicology*. Pergamon Press, Amsterdam, The Netherlands, 1263 pp.
- Kilham, S.S., Kreeger, D.A., Goulden, C.E., Lynn, S.G., 1997. Effects of algal food quality on fecundity and population growth rates of *Daphnia*. *Freshwater Biol.* 38, 639–647.
- Kleppel, G.S., Burkart, C.A., Houchin, L., 1998. Nutrition and the regulation of egg production in the calanoid copepod *Acartia tonsa*. *Limnol. Oceanogr.* 43, 1000–1007.
- Lampert, W., Sommer, U., 1997. *Limnology*. Oxford University Press, Oxford, UK, 382 pp.
- Legendre, P., Legendre, L., 1998. *Numerical Ecology*, second ed. Elsevier Science BV, Amsterdam, The Netherlands, 853 pp.
- Lehman, J.T., 1988. Selective herbivory and its role in the evolution of phytoplankton growth strategies. In: Sandgren, C.D. (Ed.), *Growth and Reproductive Strategies of Freshwater Phytoplankton*. Cambridge University Press, Cambridge, UK, pp. 134–174.
- Loladze, I., Kuang, Y., Elser, J.J., 2000. Stoichiometry in producer-grazer systems: linking energy flow with element cycling. *Bull. Math. Biol.* 62, 1137–1162.
- Malchow, H., 1994. Non-equilibrium structures in plankton dynamics. *Ecol. Model.* 75, 123–134.
- McGillicuddy, D.J., McCarthy, J.J., Robinson, A.R., 1995. Coupled physical and biological modelling in the North Atlantic. 1. Model formulation and one-dimensional bloom processes. *Deep-Sea Res. I* 42, 1313–1357.
- Mitra, A., Flynn, K.J., Fasham, M.J.R., 2007. Accounting for grazing dynamics in nitrogen-phytoplankton-zooplankton models. *Limnol. Oceanogr.* 52, 649–661.
- Mulder, K., Bowden, W.B., 2007. Organismal stoichiometry and the adaptive advantage of variable nutrient use and production efficiency in *Daphnia*. *Ecol. Model.* 202, 427–440.
- Muller-Navarra, D.C., Brett, M.T., Liston, A., Goldman, C.R., 2000. A highly unsaturated fatty acid predicts biomass transfer between primary producers and consumers. *Nature* 403, 74–77.
- Muller-Navarra, D.C., Brett, M.T., Park, S., Chandra, S., Ballantyne, A.P., Zorita, E., Goldman, C.R., 2004. Unsaturated fatty acid content in seston and tropho-dynamic coupling in lakes. *Nature* 427, 69–72.
- Omlin, M., Brun, P., Reichert, P., 2001. Biogeochemical model of Lake Zurich: sensitivity, identifiability and uncertainty analysis. *Ecol. Model.* 141, 105–123.
- Orcutt, J.D., Porter, K.G., 1983. Diel vertical migration by zooplankton-constant and fluctuating temperature effects on life-history parameters of *Daphnia*. *Limnol. Oceanogr.* 28, 720–730.
- Park, S., Brett, M.T., Muller-Navarra, D.C., Goldman, C.R., 2002. Essential fatty acid content and the phosphorus to carbon ratio in cultured algae as indicators of food quality for *Daphnia*. *Freshwater Biol.* 47, 1377–1390.
- Persson, J., Brett, M.T., Vrede, T., Ravet, J.L., 2007. Food quantity and quality regulation of trophic transfer between primary producers and a keystone grazer (*Daphnia*) in pelagic freshwater food webs. *Oikos* 116, 1152–1163.
- Polis, G.A., Sears, A.L.W., Huxel, G.R., Strong, D.R., Maron, J., 2000. When is a trophic cascade a trophic cascade? *Trends Ecol. Evol.* 15, 473–475.
- Ravet, J.L., Brett, M.T., 2006. Phytoplankton essential fatty acid and phosphorus content constraints on *Daphnia* somatic growth and reproduction. *Limnol. Oceanogr.* 51, 2438–2452.
- Richman, M.B., 1986. Rotation of principal components. *Int. J. Climatol.* 6, 293–335.
- Ross, A.H., Gurney, W.S.C., Heath, M.R., 1994. A comparative study of the ecosystem dynamics of four fjords. *Limnol. Oceanogr.* 39, 318–343.
- Roy, S., Chattopadhyay, J., 2007. The stability of ecosystems: a brief overview of the paradox of enrichment. *J. Biosci.* 32, 421–428.

- Sommer, U. (Ed.), 1989. *Phytoplankton Ecology: Succession in Plankton Communities*. Springer-Verlag, Berlin, Germany, p. 369.
- Sterner, R.W., Elser, J.J., 2002. *Ecological Stoichiometry: The Biology of Elements from Molecules to the Biosphere*. Princeton University Press, Princeton, NJ, USA, 584 pp.
- Sterner, R.W., Hessen, D.O., 1994. Algal nutrient limitation and the nutrition of aquatic herbivores. *Annu. Rev. Ecol. Syst.* 25, 1–29.
- Sterner, R.W., Elser, J.J., Hessen, D.O., 1992. Stoichiometric relationships among producers, consumers and nutrient cycling in pelagic ecosystems. *Biogeochemistry* 17, 49–67.
- Van Donk, E., Lurling, M., Hessen, D.O., Lokhorst, G.M., 1997. Altered cell wall morphology in nutrient-deficient phytoplankton and its impact on grazers. *Limnol. Oceanogr.* 42, 357–364.
- Vanderploeg, H.A., Paffenhof, G.A., Liebig, J.R., 1988. Diaptomus versus net phytoplankton—effects of algal size and morphology on selectivity of a behaviorally flexible, omnivorous copepod. *Bull. Mar. Sci.* 43, 377–394.
- Vanderploeg, H.A., Paffenhof, G.A., Liebig, J.R., 1990. Concentration-variable interactions between calanoid copepods and particles of different food quality: observations and hypotheses. In: Hughes, R.N. (Ed.), *Behavioural Mechanisms of Food Selection*. NATO ASI Series, Series G: Ecological Sciences. Springer-Verlag, New York, NY, USA, pp. 595–613.
- Wetzel, R.G., 2001. *Limnology: Lake and River Ecosystems*, third ed. Academic Press, New York, NY, USA, 1006 pp.